

THESIS

OPERATIONAL RADIATION SAFETY CONSIDERATIONS DURING SUPERFICIAL  
X-RAY TREATMENT FOR VETERINARY APPLICATIONS

Submitted by

Ashutosh Singh

Department of Environmental and Radiological Health Sciences

In partial fulfillment of the requirements

For the Degree of Master of Science

Colorado State University

Fort Collins, Colorado

Fall 2021

Master's Committee:

Advisor: Del Leary

Co-Advisor: Thomas Johnson

Kathryn Wotman

Copyright by Ashutosh Singh 2021

All Rights Reserved

## ABSTRACT

### OPERATIONAL RADIATION SAFETY CONSIDERATIONS DURING SUPERFICIAL X-RAY TREATMENT FOR VETERINARY APPLICATIONS

This study was conducted to determine whether the scatter x-ray emission during a superficial radiation treatment (SRT) using the SRT-100™ result in a significant occupational dose to veterinary personnel present in the room during treatment. Measurements were taken for 50, 70, and 100 kV x-ray for 9 different SRT-100 applicators. The exposure rates at the surface of solid water phantom (SWP) phantom ranged from 3.9 mR/hr for applicator #2 to 396 mR/hr for CB18 for 50 kV, from 41 mR/hr to 2,880 mR/hr for 70 kV, and from 235 mR/hr to 7,500 mR/hr, for 100 kV, respectively. A heat map of scatter x-ray around the x-ray source was generated for 50, 70, and 100 kV at 25 cm and 75 cm above the SWP surface plane. The highest measured exposure rate was at 0.5 m from the applicator and was 76.8 mR/hr at 25 cm above SWP and 33.6 mR/hr at 75 cm above the SWP for 50 kV. Exposure rate values at same locations were 192 mR/hr and 96 mR/hr for 70 kV, and 389 mR/hr and 194 mR/hr for 100 kV, respectively. A horse phantom was utilized to generate a spatial dose profile at 1m for 50, 70, and 100 kV and it was discovered that backscatter emission has an angular response. Residence time for veterinary staff to exceed 10% of quarterly dose limits were calculated for 50, 70, and 100 kV and distances ranging from 0.5m to 2.5 m. These values ranged from a minimum of 24 min for 100 kV at 0.5m to a maximum of 7,813 min for 50 kV at 2.5 m. Minimum distance from the applicator for exposure rates below 2 mR/hr were calculated to be 1.78, 2.52, and 3.45 m, for 50, 70, and 100 kV, respectively.

## ACKNOWLEDGEMENTS

This thesis would not have been possible without the guidance of my advisory committee members. I would like to thank Dr. Kathryn Wotman for getting this project initiated, and Dr. Tom Johnson for providing his input and suggestions throughout my research work. I would like to especially thank Dr. Del Leary for being my mentor and research advisor. I am grateful to him for sharing his knowledge of health physics, resources of the medical physics lab, and his time. Above all, I thank him for the patience he has and for constantly pushing me towards the finish line.

I would also like to thank the United States Army's AMEDD Center and School for selecting me for the Long Term Health Education & Training program and for providing me the opportunity to pursue my Master's degree at the Colorado State University.

I am grateful to Dr. Alex Brandl and Dr. Ralf Sudowe for being excellent professors and for teaching during challenges of the pandemic. I would also like to thank my fellow health physics graduate students, who helped me transition back into classroom learning after many years.

Finally, I would like to thank my wife Lauren, for her immense love and support throughout the last two years in Colorado. This would not have been possible without you and our son, Ishaan keeping me motivated through trying times.

## TABLE OF CONTENTS

ABSTRACT.....	ii
ACKNOWLEDGEMENTS.....	iii
LIST OF TABLES.....	vi
LIST OF FIGURES.....	vii
INTRODUCTION.....	1
LITERATURE REVIEW.....	3
Superficial Radiation Treatment.....	3
Personal Dosimeters.....	5
MATERIALS AND METHODS.....	10
SRT-100.....	10
Detector.....	12
GafChromic Film.....	13
RESULTS.....	16
Detector Angular Response.....	16
Effect of Applicator Size on Exposure Rates.....	19
Scatter Exposure Rate Heat Map for SRT-100.....	22
Horse Phantom Backscatter.....	32
Percentage Depth Dose Curves.....	35
DISCUSSION.....	40
Detector Orientation Dependence.....	40
Exposure with Varying Energy and Applicator Size.....	40

Exposure and Occupational Time Limits .....	42
Energy Response Correction Factor .....	44
Angular Scattering from Horse Head Phantom .....	45
CONCLUSIONS.....	52
REFERENCES .....	54
APPENDIX A.....	58
APPENDIX B .....	59
APPENDIX C .....	60
APPENDIX D.....	61
APPENDIX E .....	62
APPENDIX F.....	63
APPENDIX G.....	64
LIST OF ACRONYMS .....	67

## LIST OF TABLES

Table 1: Treatment parameters for SRT-100 .....	11
Table 2: Normalized Angular Response of Detector - Vertical.....	16
Table 3: Normalized Angular Response of Detector -Horizontal .....	18
Table 4: Applicator dimensions .....	19
Table 5: Estimated Dose Rates (mrem/hr) at various distance from applicator .....	42
Table 6: HVL, attenuation coefficients, and attenuation factor broad beam x-ray.....	43

## LIST OF FIGURES

Figure 1: SRT-100™ Superficial Radiation Therapy System .....	10
Figure 2: Control panel for SRT-100.....	11
Figure 3: Gafchromic 50 kV exposures for generation of calibration curve .....	14
Figure 4: Depth-dose profile of 50 kV exposure of 1 min with a 2 cm applicator .....	15
Figure 5: Measurement of Detector Angular Response – Vertical.....	17
Figure 6: Measurement of Detector Angular Response – Horizontal.....	18
Figure 7: Measurement of exposure rate for various applicators .....	20
Figure 8: Exposure rate vs Applicator size at the surface.....	21
Figure 9: Exposure rate vs Applicator size at 0.5m.....	21
Figure 10: Measurements for the Scatter Heat Map around SRT-100 .....	22
Figure 11: Scatter Exposure Rate Heat Map for 50 kV at Z=25cm.....	23
Figure 12: Scatter Exposure Rate Heat Map for 50 kV at Z=75cm.....	23
Figure 13: Scatter Heat Map for 70kV at Z=25cm.....	25
Figure 14: Scatter Heat Map for 70 kV at Z=75cm.....	25
Figure 15: Scatter Exposure Rate Heat Map for 100 kV at Z=25cm.....	26
Figure 16: Scatter Exposure Rate Heat Map for 100 kV at Z=75cm.....	26
Figure 17: Calculation of Angle Subtended at Applicator by Detector.....	27
Figure 18: Scatter Exposure Rate Profile for 50 kV x-rays along X Axis.....	29
Figure 19: Scatter Exposure Rate Profile for 50 kV x-rays along Y Axis.....	29
Figure 20: Scatter Exposure Rate Profile for 70 kV x-rays along X Axis.....	30
Figure 21: Scatter Exposure Rate Profile for 70 kV x-rays along Y Axis.....	30

Figure 22: Scatter Exposure Rate Profile for 100 kV x-rays along X Axis.....	31
Figure 23: Scatter Exposure Rate Profile for 100 kV x-rays along Y Axis.....	31
Figure 24: Horse Phantom Backscatter Experiment Layout.....	32
Figure 25: Backscatter Exposure Rates for Horse Phantom at 0.5m.....	33
Figure 26: Backscatter Exposure Rates for Horse Phantom at 1m.....	33
Figure 27: Backscatter Profile for the Horse Phantom at 1m.....	34
Figure 28: Percentage Depth-Dose Curve Generation Experiment.....	36
Figure 29: Percentage Depth-Dose Curve for 1.5 cm Applicator.....	37
Figure 30: Percentage Depth-Dose Curve for 2.0 cm Applicator.....	37
Figure 31: Percentage Depth-Dose Curve for 2.5 cm Applicator.....	38
Figure 32: Percentage Depth-Dose Curve for 3.0 cm Applicator.....	38
Figure 33: Percentage Depth-Dose Curve for 5.0 cm Applicator.....	39
Figure 34: Residence time in treatment room without any PPE.....	43
Figure 35: Residence time in treatment room with lead apron.....	44
Figure 36: Energy corrected residence time in treatment room with lead apron.....	45
Figure 37: Optimal Location for Veterinary Personnel during SRT .....	46
Figure 38: Angular dependence of residence time at 1 m .....	47
Figure 39: Dose Rate vs Distance for 50 kV .....	48
Figure 40: Dose Rate vs Distance for 70 kV .....	48
Figure 41: Dose Rate vs Distance for 100 kV .....	49
Figure 42: Estimated Distance from Applicator for 2 mR/hr Exposure Rate.....	50

## INTRODUCTION

Treatment of dermatological diseases using x-rays commenced soon after their discovery in 1895 by Wilhelm Roentgen. Use of x-rays as a therapy to cure a variety of cutaneous diseases had been studied and was an accepted practice by 1920s (MacKee, 1927). Radiation therapy has been used for treatment of skin cancers in humans, most notably, Basal cell carcinoma (BCC) and Squamous cell carcinomas (SCC). Radiation therapy is employed most commonly either for lesions that have been removed surgically or that have recurred. Radiation treatment can also be the primary treatment if the lesion is located near eyes or lips (Halpern, 1997).

X-rays used in dermatological applications are categorized based on their energy. Least penetrating x-rays with energies less than 20 kV are referred to as Grenz rays or ultrasoft x-rays and are used in treatment of benign dermatoses. Treatment of most epithelial cancers are performed using x-rays between 60-100 kV and are referred to as superficial x-rays. Higher energy x-rays are called orthovoltage or hard x-rays and can have energy up to 250 kV (Goldschmidt, Breneman, & Breneman, 1994).

One of the primary advantages of using Superficial Radiation Treatment (SRT) with x-rays is that dose to critical organs is not a concern due to poor penetrating characteristics of low energy x-rays. Therefore, SRT has become treatment modality of choice for dermatological applications. However, the application of SRT in veterinary patients has been extremely limited. Most SRT x-ray therapies have been used on small animal patients that were anesthetized during the treatment. Deep sedation of the animal has the benefit of patient immobility during treatment, but it requires an anesthesiologist team and constant monitoring of the patient before, during, and after the procedure.

Complete sedation using general anesthesia is a challenging endeavor for a large equine patient due to the longer preoperative checkup, post-operative recovery, and requires more resources at a veterinary facility due to higher possibility of complications. Standing sedation for horses has been found to be a safe and effective alternate to general anesthesia (Vigani & Garcia-Pereira, 2014). However, standing sedation requires the presence of a veterinary staff near the horse to monitor it and ensure it does not move during the SRT treatment when the x-ray unit is on. SRT x-rays presents a radiation safety challenge due to scatter x-rays being emitted and has not been previously evaluated.

The primary purpose of this study was to characterize the scatter x-ray emission in the vicinity of SRT-100™ Superficial Radiation Treatment for various x-ray energies and applicator sizes in order to minimize the dose to the veterinary staff. It is hypothesized that veterinary staff can be present in the room during SRT procedure without receiving a significant dose from scatter x-ray. A secondary purpose was to validate the percentage depth-dose (PDD) values reported by the manufacturer.

## LITERATURE REVIEW

### Superficial Radiation Treatment

Superficial Radiation Treatment utilizing x-rays to treat skin carcinomas in humans has been employed by dermatologists since the 1950s. SRT using soft x-rays (50-100 kV) provides many advantages such as simplicity of use and being cost effective. The SRT has been widely accepted in the field of dermatology for skin treatment of humans (Sheu, Powers, & Lo, 2015).

SRT using x-rays offer several advantages over the competing therapies such as an electron beam which has sharp field edges and deeper penetration. SRT involves the use of applicators (either cylindrical or cone shaped) of various sizes that are attached to the x-ray tube and target the skin. Selecting the appropriate applicator is critical, as it determines the field size of x-ray and the source to skin distance (SSD) the incident dose rate to the skin (Goldschmidt, Breneman, & Breneman, 1994). In addition, the applicator size also determines scatter radiation emission and is therefore important to radiation safety. Typically, the incident dose on the tumor of depth  $D$  is calculated using the thumb rule of  $D_{1/2}$ , (50% depth dose) of the x-ray beam to tumor depth. Using the thumb rule results in most of the radiation being delivered to the tumor while sparing the healthy tissue.

Use of superficial low kV x-ray treatment has also been studied as alternate to High Dose Rate (HDR) brachytherapy as part of an intraoperative radiotherapy (IORT) modality (Schneider, Clausen, Tholking, Wenz, & Abo-Madyan, 2014). Either HDR or high energy electron beam requires the patient be transported to a treatment room with specific radiation shielding protection and no additional staff be present during that therapy. The radiation protection requirements for electron beam treatment makes low kV SRT a viable treatment

option during IORT (Guo, et al., 2012). X-ray SRT has also been used in conjunction with other methods to treat chronic skin diseases in humans. In one such study, SRT was used along with Hydroxychloroquine to treat morphea profunda (MP) (Li, Zhang, Wang, & Chen, 2019). Morphea is a chronic inflammatory disease that causes sclerosis of skin and the underlying subcutaneous tissues. Morphea profunda is one of the rare variants of this disease with an unknown etiology and etiopathogenesis. During the treatment, 100 kV x-rays were targeted at 1.2 cm in skin to deliver 4 fractionated doses of 12.5 Gy, and 17.1 Gy for one month each, along with 400 mg/day of Hydroxychloroquine. According to the authors, the treatment provided a positive clinical effect in a short time with fewer side effects than the control, and the non-invasive and painless aspect of SRT contributed to patient compliance.

The 2 and 5 year recurrence rates for basal cell carcinomas treated with SRT were 2% and 4%, and 1.8% and 5.8% for squamous cell carcinomas (Cognetta, et al., 2012). SRT was shown to be a viable option for primary treatment of nonaggressive, carcinomas for patients that either decline surgery, have comorbidities, or due to significant cosmetic or functional limitations. SRT-100 x-ray unit was used to as a post-surgical treatment after removal of keloid scars. The recurrence rate for these scars is approximately 70%, which was reduced to 10.4% within 12 months and 12.7% after 18 months with SRT (Berman, et al., 2020).

Most of the studies related to use of x-ray SRT have focused on the application of dose to the target site, analysis of dose produced by various x-ray units, effect of beam quality and dose distribution etc. and their agreement with computer models (Al-Ghorabie, 2015), (Sergei, Butorov, & Shevchenko, 2019). Radiation safety of the operator or other staff present in the room is not a factor for these treatment since human patients are compliant during the treatment and change in target site due to patient movement does not occur. There have been limited

studies of using x-ray SRT on veterinary patients compared to the number of human dermatological studies. SRT has been used to treat chronic superficial keratitis (CSK) using 15 kV x-rays in dogs (Allgoewer & Hoecht, 2010) Using soft x-rays was found to be a safe and effective treatment option for dogs with severe and advanced CSK as compared to traditional treatment modality of using Sr-90 irradiation. Allgoewer & Hoecht applied SRT while dogs were under deep sedation. However, there might be situations where a complete sedation of the animal is not possible and would require a veterinarian staff to be present in the vicinity of the animal. Treatment of equine veterinary patients would be one such situation where the scatter x-ray exposure to the staff becomes challenge from a radiation safety aspect. Scatter radiation is a significant radiation safety challenge in procedures that require presence of humans in the vicinity of patients when the x-ray is being used. This is typically observed in interventional radiology procedures where physicians must be extremely close to the patient and consequently get scatter radiation dose to the whole body and to the head and neck (Fetterly, Schueler, Grams, & Sturchio, 2017).

### Personal Dosimeters

Historically, radiation safety programs all over the world have relied on use of passive dosimeters that integrated the dose over a period (month, quarter, year etc.) in order to monitor individual doses. These passive dosimeters were film badges, thermo-luminescence dosimeters (TLD), or optically stimulated dosimeters (OSL). Passive dosimeters require them to be sent to a processing lab to obtain the dose accumulated during the wear period. One difference is that TLDs can have the total exposure read only once compared to OSLs that allow for multiple readings of the aggregate exposure.

Passive dosimeters were used in this study in conjunction with either an area monitor or another portable rate meter with an alarm function that provided real time information about dose accumulated or an increase in dose rate. This information was important to identify dose rate/total dose levels that exceeded a critical limit or indicated an emergency, where radiation workers might be exposed to high radiation levels.

Electronic personal dosimeters (EPD) have alleviated key shortcomings of the passive dosimeters providing a real time estimate of accumulated dose and can also serve the alarm function by monitoring the dose rates (Krzanovic, et al., 2017). The working principle of EPDs is based on either using a Geiger-Muller tube or silicon (Si) diode. There are some EPDs that use an inorganic scintillator such as thallium doped cesium iodide [CsI(Tl)] for dose measurement. Krzanovic et al, studied 10 various types of EPDs after being irradiated with a range of gamma and x-rays and assessed their accuracy, dose rate linearity, energy, and angular response. It was discovered that for 33 keV x-ray beam, only 3 EPDs performed according to the test standards. The poor performance of EPDs in low energy x-ray fields was observed by (Texier, Itie, Serviere, Gressier, & Bolognese-Milsztajn, 2001) and (Ginjaurme, et al., 2007) who discovered that only 12 out of 31 photon and beta-photon dosimeters measured photons less than 50 kV. Dose response is an important limitation during use of EPDs in a medical application where exposure from low kV photons is expected.

Radiation workers in South Korea wear a TLD as their official dosimeter for record. A study was undertaken in 2016 to assess the performance of 6 active personal dosimeters (APDs) in comparison to the TLDs that the workers were wearing (Lee, Won, & Kang, 2017). These APDs were tested for dose and dose-rate response, and photon energy response against the TLDs. The photon energy response was measured for irradiation with a  $^{137}\text{Cs}$  source (662 keV)

and x-rays ranging in average energy from 20 keV to 118 keV. They discovered that only 3 APDs performed satisfactorily in all tests when compared to the TLDs, with 2 EPDs failing the deep tissue dose test due to their inability to measure photons with energy less than 50 keV. It was their recommendations that APDs can be used in place of TLDs as they provided accurate data, however there were other factors like malfunction, battery life, correction factor applications, that needed to be considered before switching to APDs.

Dose received from scatter x-ray radiation to nearby personnel is of particular concern during the interventional radiology (IR), where the beam on time for the procedure can be substantial and due to the presence of medical staff around the patient. The occupational dose limit to the lens of eye is currently 150 mSv/year. However, based on latest epidemiological studies, the International Commission of Radiation Protection (ICRP) has issued guidelines to reduce the occupational exposure to the eye from 150 mSv/year to 20 mSv/year averaged over a 5-year period with a maximum of 50 mSv being received in any one year (ICRP, 2012). The NCRP has recommended 50 mSv per year to the lens of the eye (NCRP, 2016).

As a result of this reduced threshold, there was a renewed interest in exploration of EPDs to assess the dose to the lens of eye and a study was conducted in Ireland (Masterson, et al., 2019). Various EPDs were compared with 2 LiF TLDs, exposed to scattered x-ray from a polymethylmethacrylate phantom (PMMA) interrogated with 50-81 kV x-rays from a Siemens C-Arm system. The EPDs tested in the study had an energy response that overestimated the dose between 2 and 9% when compared to the calculated dose from a standard ion chamber. In addition, the EPDs had a relative response within 6% across the 50-81 kV energy spectrum, thus indicating a relatively flat energy response.

Radiation dose rate is another important factor that can affect the response of EPDs. Investigators examined the effect of various dose rate on the response of EPDs (McCaffrey, Shen, & Downton, 2008). Air kerma measurements were taken and converted to personal dose equivalents using the conversion factors from ICRU Report 57 (ICRU, 1998). Siemens Mk 2.3 EPD provided the flattest response and had the smallest difference between in air vs water phantom measurements. It also maintained the most consistent response over the range of dose rates with the dose variation being less than 5%. The Siemens Mk 2.3 was also noteworthy for its ability to accurately detect the 15.1 average kV x-ray as claimed.

In addition to countries in European Union like Germany, UK, Greece, and Canada, the regulatory authorities in United States allow the use of EPDs for official dose of record. (Ortega, Ginjaume, Hernandez, Villanueva, & Amor, 2001) The US Nuclear Regulatory Commission (NRC), in 10 CFR part 34 §34.47(a) states that during radiographic operations, radiographers and radiographer's assistants must wear "a direct reading dosimeter, an operating alarm ratemeter, and a personnel dosimeter that is processed and evaluated by an accredited National Voluntary Laboratory Accreditation Program (NVLAP) processor". Although, processing was not explicitly defined by the NRC, it noted that processing is necessary with film, TLD, and OSL dosimeters. It also noted that NVLAP accreditation does not certify or accredit the dosimetry devices themselves, but instead provides a level of quality assurance during the read-out process of the dosimeters. NRC, in response to a petition by the American Society for Nondestructive Testing, amended its requirements to include digital output personnel dosimeters to satisfy the personnel dosimetry requirements in § 34.47(a) and similar provisions in 10 CFR parts 36 and 39, effective from June 16, 2020, (Federal Register, 2020). NRC in its rule making used the term 'digital output personnel dosimetry' to denote multiple terms like 'improved individual

monitoring devices’, ‘electronic personnel monitoring dosimeters’, ‘electronic dosimeters’, and ‘digital personnel dosimeters’.

Siemens MK2+ is one of the most scientifically evaluated EPDs. The latest version is known as the Thermo Scientific EPD TruDose Electronic Dosimeter (Thermo Fisher Scientific, 2021) marketed by Thermo-Fisher Scientific Inc. There are 3 variants of the TrueDose EPD with specific capabilities, NG is capable of Neutron and gamma detection, G is for gamma radiation detection, and BG variant can detect both beta and gamma radiations.

TrueDose G variant has an effective range of dose of 0.1 mrem to greater than 1000 rem for deep dose equivalent ( $H_p(10)$ ), and 5 mrem to 1000 rem for skin dose equivalent ( $H_p(0.07)$ ), respectively. Very few EPDs have the capability to measure skin dose. The accuracy for deep dose equivalent is  $\pm 5\%$ , and for skin dose equivalent its  $\pm 15\%$ .

The LCD screen display provides a real time dose reading and the alarm function can indicate excessive dose or dose rate. In addition to having a desktop reader to download and review the dose data, TrueDose G EPD also has Bluetooth capability to a central monitoring facility using remote telemetry and can be part of a command and control center.

## MATERIALS AND METHODS

### SRT-100

This study utilized an SRT-100™ Superficial Radiation Therapy System (Figure 1) manufactured by Sensus Healthcare LLC, Boca Raton, FL 33487, USA. The SRT-100 therapy unit has been approved by the US Food & Drug Administration for the treatment of non-melanoma skin cancer and keloids (Sensus Healthcare, 2021).



Figure 1: SRT-100™ Superficial Radiation Therapy System

Table 1: Treatment parameters for SRT-100

x-ray kV	HVL (mm Al)	Tube Current (mA)
50	0.43	10
70	1.04	10
100	1.87	8

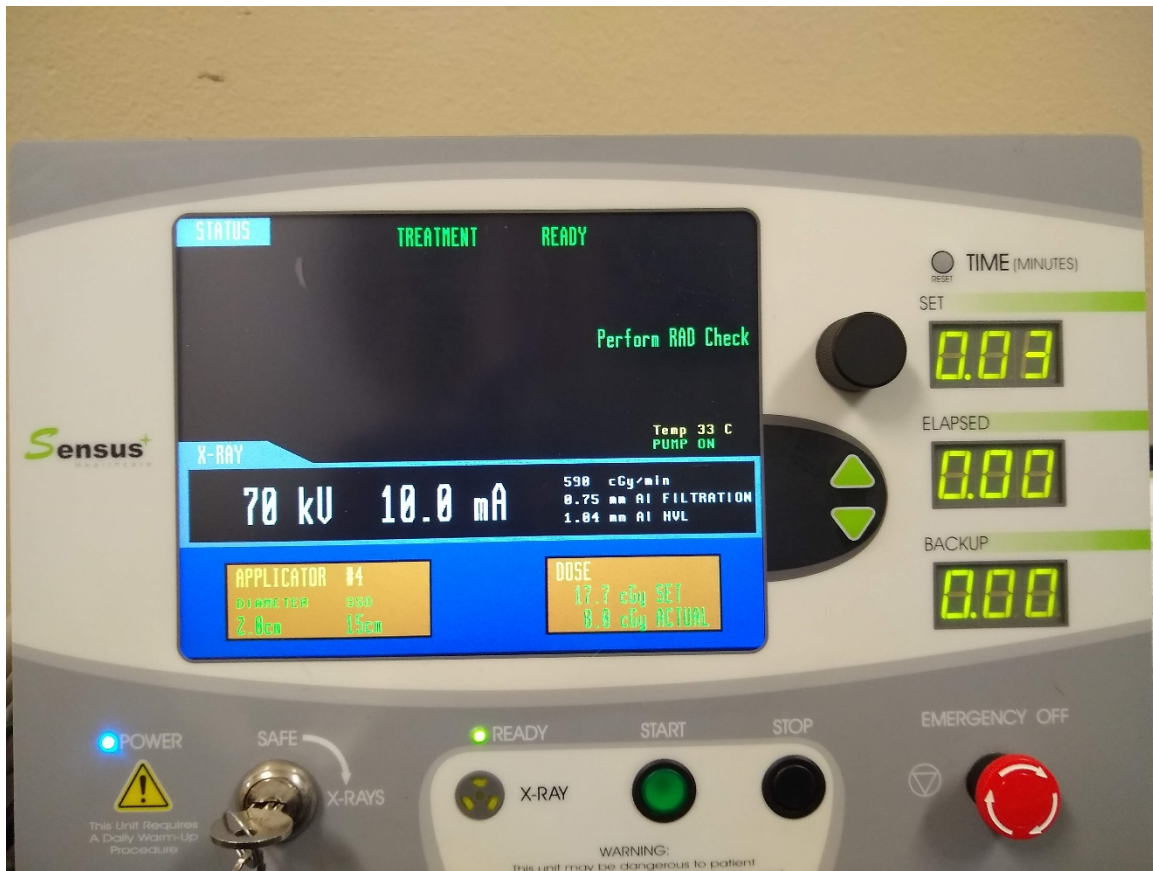


Figure 2: Control panel for SRT-100

SRT-100 has the 3 x-ray energies available for treatment, 50, 70, and 100 kV as shown in Table 1. The x-ray tube filtration and current are preset for the kV selected. Treatment parameters selection is made on the control panel as shown in Figure 2. SRT-100 automatically recognizes the applicator being used and displays the applicator number, diameter, and source to

skin distance (SSD) for that applicator. The SRT-100 also, displays the kV selected, dose rate for the kV and applicator in cGy/min, tube filtration and Half value layer (HVL) in mm of Al. Treatment time can be selected from 0.01 min to 3.0 min, in increments of 0.01 min. Total dose selected for the procedure is displayed and elapsed time and dose delivered is continually displayed after initiation of treatment. SRT-100 is a water-cooled x-ray tube and the unit shuts off once the water temperature reaches 42°C to prevent over-heating of the tube. The unit requires a 6-minute warm cycle at the beginning of the day and a quality control procedure to ensure correct dose is being delivered during treatment.

All experiments for this study were performed in the LINAC (Linear Accelerator) room (Room number D106C) in the Radiation Oncology section at the Veterinary teaching hospital of the Colorado State University (CSU) located in Fort Collins, CO. The shielding of the LINAC room was sufficient for radiation safety purposes. Radiation measurements taken outside the room were at background level while the SRT-100 was being used at the highest kV. The SRT-100 operator completed all training requirements of the Radiation Control Office (RCO) at CSU and wore a whole-body dosimeter while conducting experiments. Administrative controls were in place to ensure no staff or member of public would enter the room while the x-ray unit was operational.

#### Detector

Exposure measurements for this study were taken using a Fluke Model 451P ion chamber survey meter. It is a handheld radiation detection device with 230 cm<sup>3</sup> active volume ionization chamber pressurized to 8 atmospheres, designed to detect gamma radiation above 25 keV (Anonymous, 2013). It was operated in the integrated data collection mode during the

experiments to calculate the exposure dose rates in mR/min or mR/hr. The handheld pressurized ion chamber used for this study has a relatively large active volume of 230 cm<sup>3</sup> compared to the thimble type ion chambers. This results in lower spatial resolution but a much better signal to noise ratio (Takata, Korosawa, & Tran, 2003). This size of this chamber was suitable for the spatial resolution required for this work.

#### GafChromic Film

Data for the percentage depth-dose (PDD) experiments were collected using 8" × 10" sheets of EBT-3 type Gafchromic™ dosimetry film. It has a proprietary 28µm thick active layer sandwiched between 2 layers of 125 µm thick matte-surface polyester substrate. The dynamic dose range of EBT-3 film was 0.1 to 20 Gy.

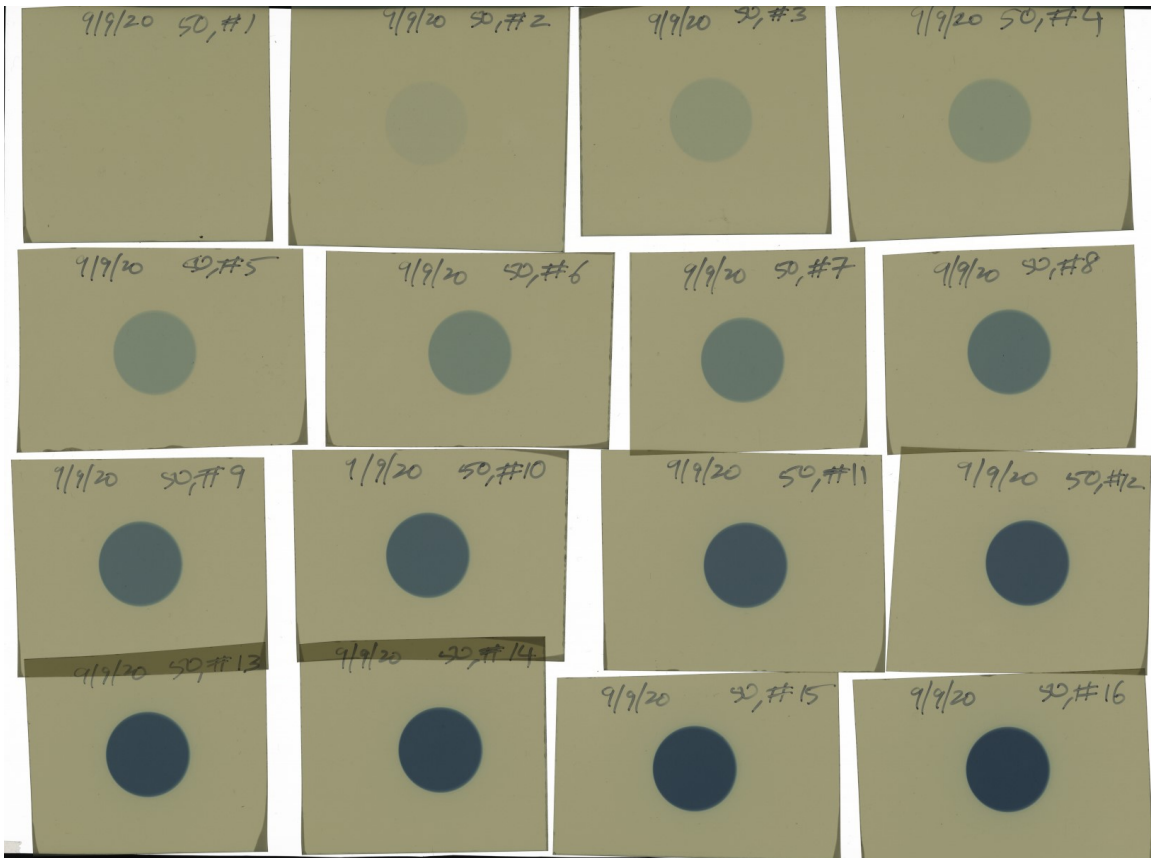


Figure 3: Gafchromic 50 kV exposures for generation of calibration curve

EBT-3 films that were exposed to x-ray were scanned using an Epson Expression 10000XL scanner (Figure 3). The scanned images were imported into the RIT Version 6.0 software to generate the calibration curve, Radiological Imaging Technology, Colorado, 80919, USA.

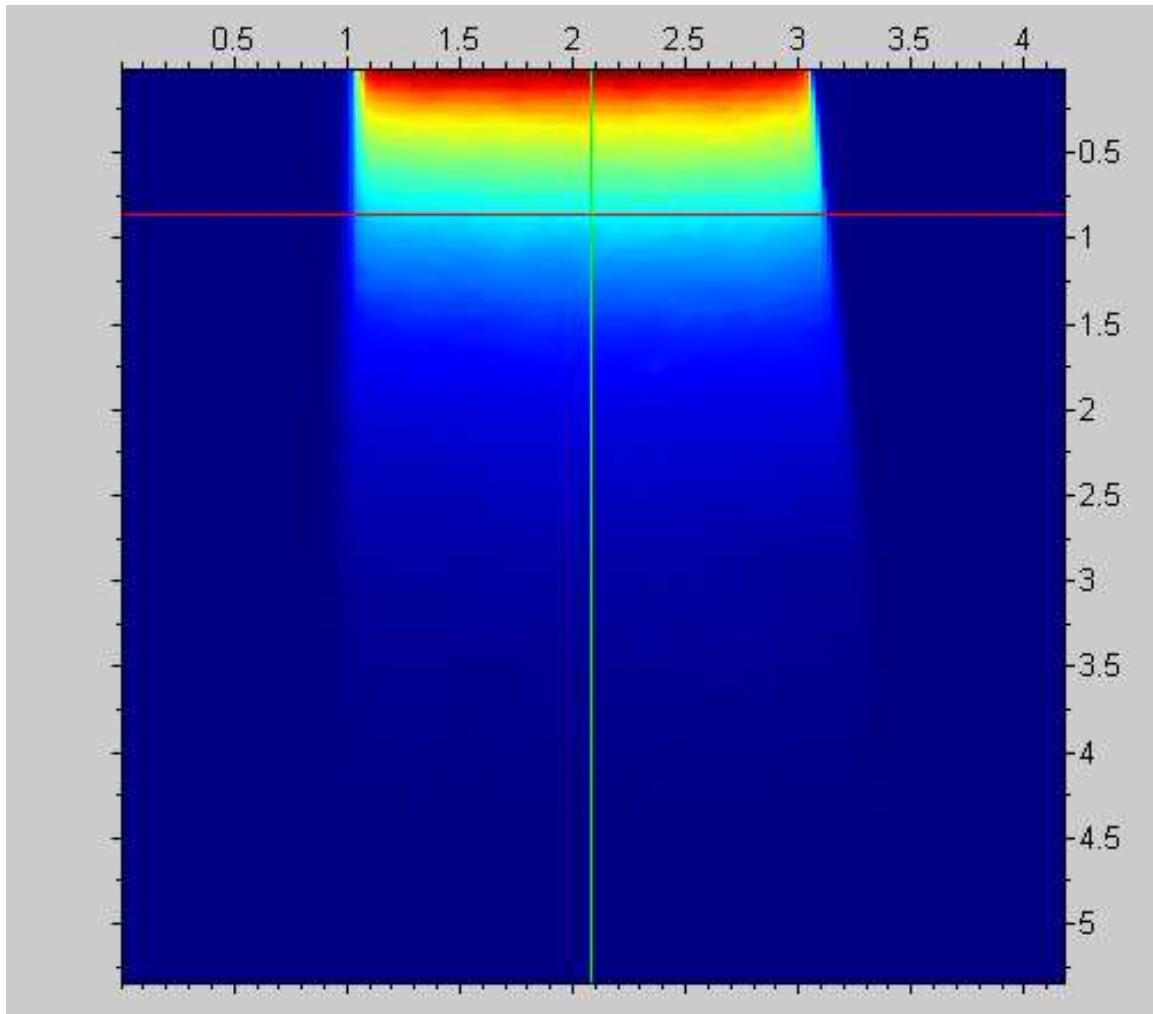


Figure 4: Depth-dose profile of 50 kV exposure of 1 min with a 2 cm applicator

In order to generate the PDD curves, EBT-3 film was sandwiched between 2 SWP blocks of 6 cm thickness and exposed to 50, 70, and 100 kV x-ray for 1 min each. Each film was scanned into the Epson scanner and a depth-dose profile generated similar to one shown in Figure 4. Raw data for the optical density were imported in a .CSV format and Excel (Microsoft Corp, WA, USA) was used to process the raw data and generate the PDD curves.

## RESULTS

### Detector Angular Response

Initial experiments were performed to assess the detector direction and orientation sensitivity on the measurement of exposure rates. The objective of these experiments was to characterize the detector orientation and directionality in order to select the detector orientation for the subsequent experiments measuring exposure rates.

In these experiments the detector was rotated with respect to the direction of SRT-100 x-ray tube at 0°, 30°, 45°, 60°, and 90°. Exposure rate measurements were taken for 30 seconds, and for beam energies at 50, 70, and 100 kV. The x-ray tube with a 2 cm diameter was incident on a 6 cm thick Solid Water Phantom (SWP) and detector was placed at 1m from the tube. The experiment layout was as shown in Figure 5 and Figure 6.

The exposure rates measurements (mR/min) for the detector in a vertical orientation are presented in Table 2. Exposure rates in mR/min were determined from the raw data and were normalized with 0° direction as 100%. The exposure rate measurements did indicate directional dependence. However, all the normalized values for the exposure rates were found to be within the accuracy of the detector of  $\pm 10\%$  (Anonymous, 2013).

Table 2: Normalized Angular Response of Detector - Vertical

Normalized Exposure Rate (%)	0°	30°	45°	60°	90°
50 kV	100	94.1	96.1	97.1	103.9
70 kV	100	95.7	96.4	100.4	98.9
100 kV	100	95.5	95.5	97.0	95.5

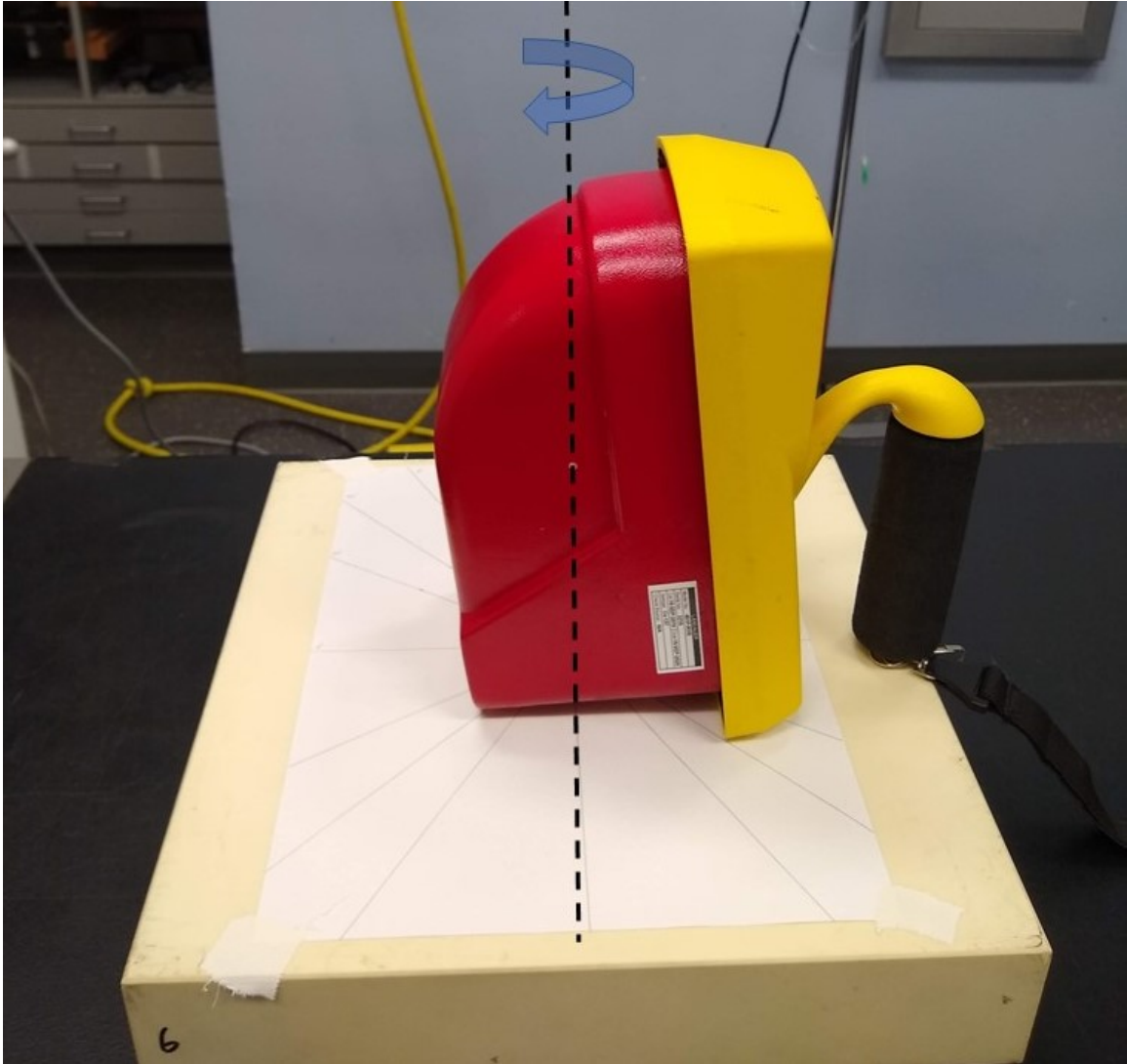


Figure 5: Measurement of Detector Angular Response – Vertical

Measurement data for the normalized angular response of the detector in a horizontal orientation are shown in Table 3. The results are similar to those observed in the vertical detector orientation, with a higher deviation from the  $0^\circ$  values than as compared to the vertical orientation. This can be attributed to the change in relative location of the active volume of the detector with respect to the Xray source. However, as with the vertical orientation the deviation was within accuracy of the detector.

Table 3: Normalized Angular Response of Detector -Horizontal

Normalized Exposure Rate (%)	0°	30°	45°	60°	90°
50 kV	100	90.9	97.0	106.1	107.7
70 kV	100	97.9	103.2	106.3	109.4
100 kV	100	99.1	100.2	103.1	107.2

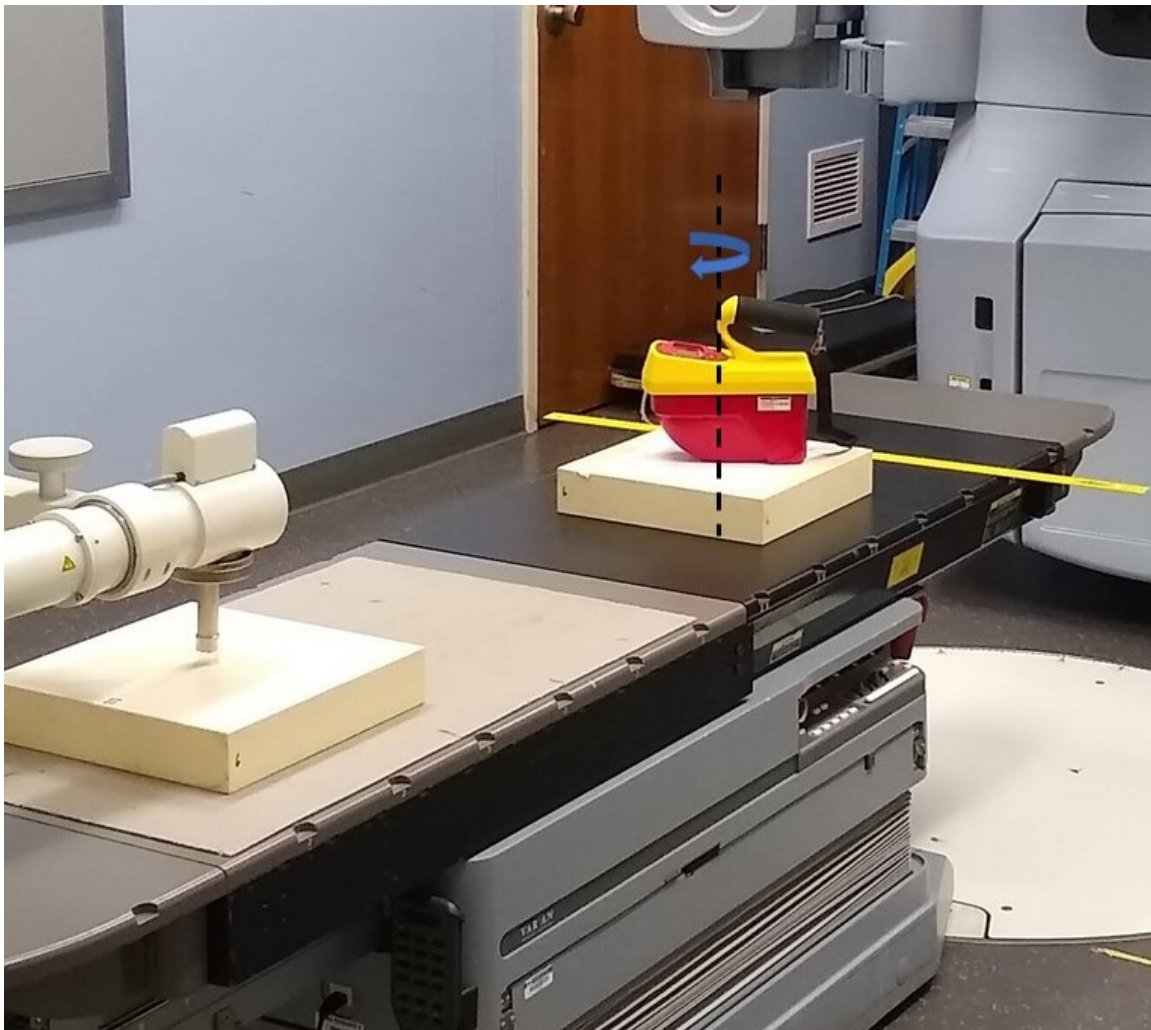


Figure 6: Measurement of Detector Angular Response – Horizontal

This characterization of the angular response of the detector was important while planning the measurement of exposure rate around the x-ray experiment where the simplicity and consistency of experimental layout during data acquisition phase was necessary.

#### Effect of Applicator Size on Exposure Rates

Experiments were conducted to study the effect of the applicator size on the exposure rates measured (mR/hr) using energies of 50, 70, and 100 kV directed at solid water phantoms (SWP) of 25 cm total thickness. Measurements were taken using a Fluke 451 detector at two distances, right next to the phantom surface (nearest face of SWP block) and at 0.5 m from the phantom surface. Each measurement was taken for 12 seconds, and results converted to mR/hr. Figure 3 shows the experimental layout for these measurements. The applicator sizes for this experiment are listed in Table 2, including the applicator number, diameter, and the source to surface distance (SSD).

Table 4: Applicator dimensions

Applicator Number	Applicator Diameter (cm)	Source to Surface Distance (cm)
#2	1.5	15
#4	2.0	15
#5	2.5	15
#6	3.0	15
#8	4.0	15
#10	5.0	15
#12	10	25
#7	18 × 8	25

Applicator #7 is a cowbell shaped ellipse with a major axis of 18 cm and a minor axis of 8 cm. Two measurements were taken for this applicator along its major and minor axes.

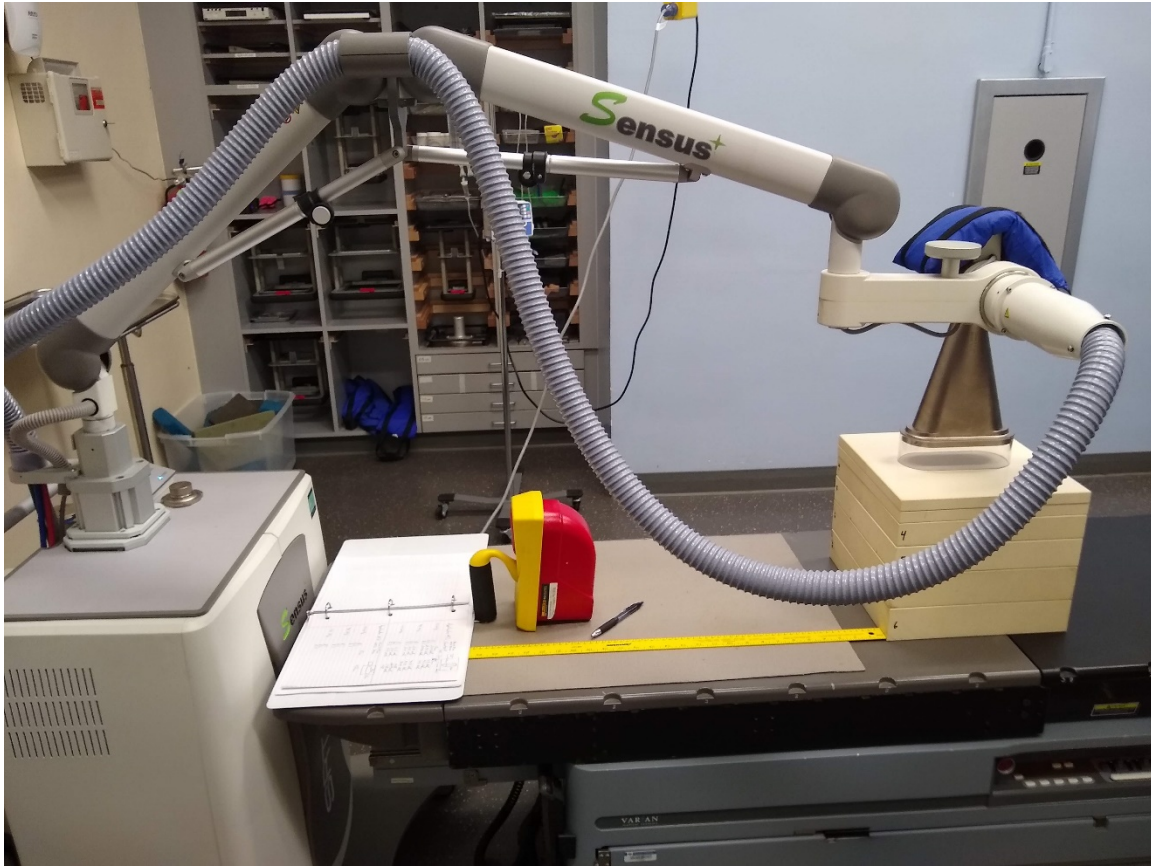


Figure 7: Measurement of exposure rate for various applicators

Results for this experiment are shown in Figure 8 for measurements taken at the surface, and Figure 5 for measurements taken at 0.5m from the SWP surface. The measurements for the cowbell shaped applicator #7 are listed as CB18 for measurement along the major axis (18 cm) and CB8 for measurement along the minor axis (8 cm). As expected, the exposure rates increased with increased beam energy for all applicators, and for measurements at the surface and at 0.5 m away from the SWP surface. The exposure rates at the surface ranged from 3.9 mR/hr for applicator #2 to 396 mR/hr for CB18 for 50 kV, from 41 mR/hr to 2,880 mR/hr for 70 kV, and from 235 mR/hr to 7,500 mR/hr, for 100 kV, respectively.

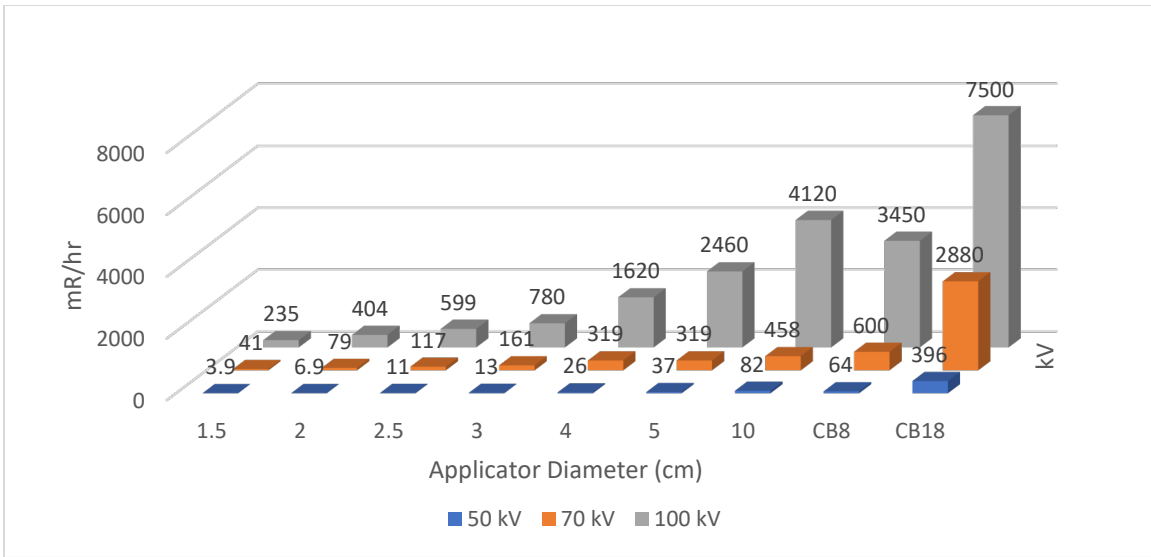


Figure 8: Exposure rate vs Applicator size at the surface

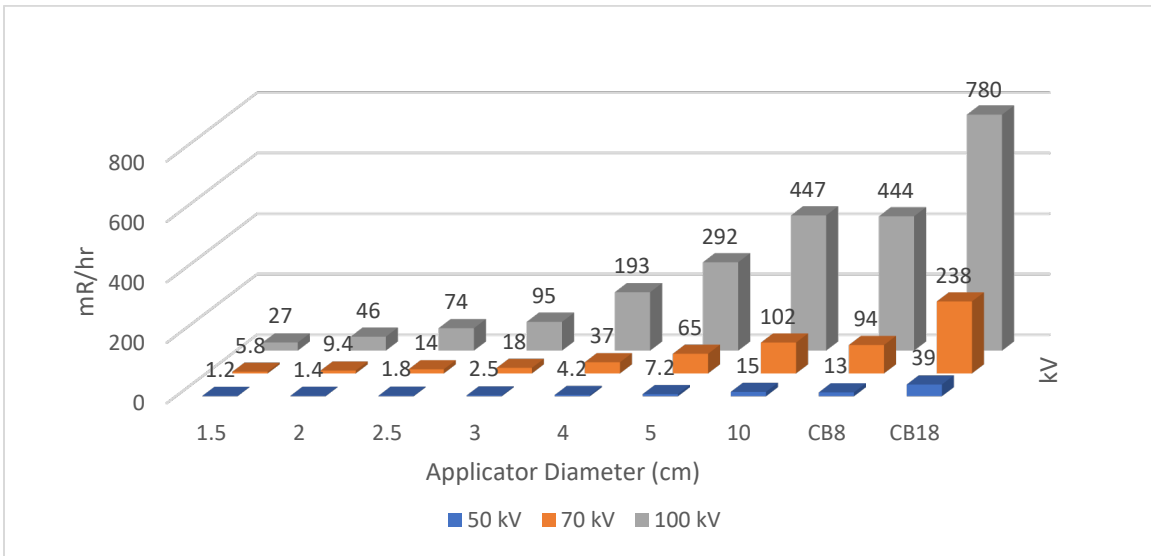


Figure 9: Exposure rate vs Applicator size at 0.5m

The exposure rates decreased significantly when the detector's distance was increased to 0.5 m away from the SWP surface. The exposure rates values for smallest and largest applicators ranged from 1.5 mR/hr to 39 mR/hr for 50 kV, from 5.8 mR/hr to 238 mR/hr for 70 kV, and 27

mR/hr to 780 mR/hr for 100 kV, respectively. The exposure rates decreased by approximately one order of magnitude by increasing the detector distance from surface of SWP to 0.5 m.

#### Scatter Exposure Rate Heat Map for SRT-100

In order to characterize scattering field of the x-ray device for safety of potential nearby personnel, a heat map of the measure exposure rate at various locations was generated. Exposure rate was measured around the x-ray tube while beam was incident on a 6 cm thick SWP with a 2 cm diameter applicator (#4). Measurements were taken in the XY plane in a  $0.5\text{m}\times 0.5\text{m}$  grid at 25 cm and 75 cm above the surface of the SWP. Scatter measurements were collected for 50, 70, and 100 kV for 15 seconds and exposure converted into exposure rates (mR/hr). The experiment layout is shown in Figure 10.



Figure 10: Measurements for the Scatter Heat Map around SRT-100

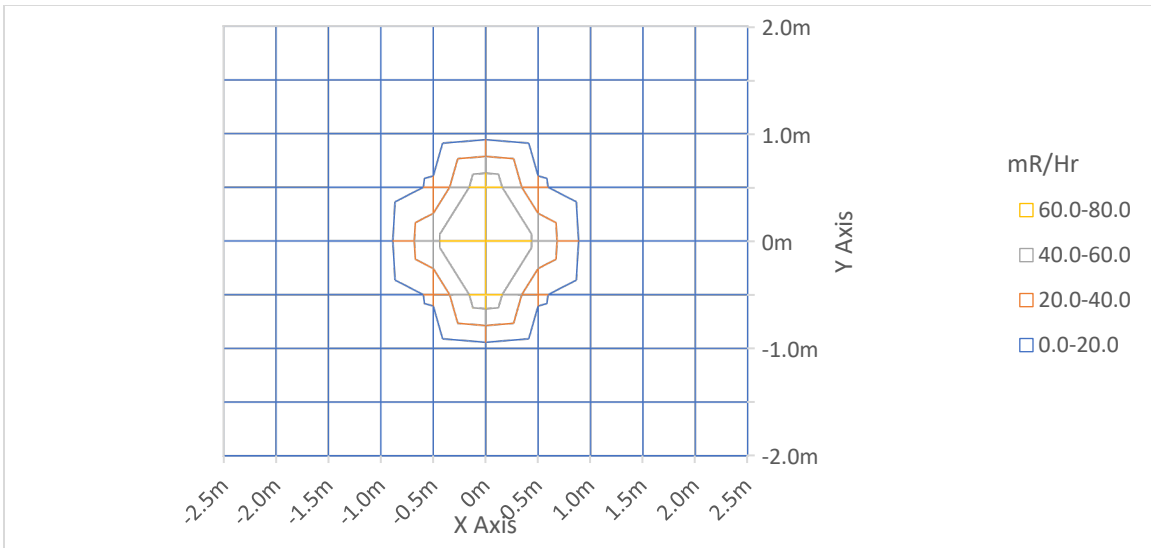


Figure 11: Scatter Exposure Rate Heat Map for 50 kV at Z=25cm

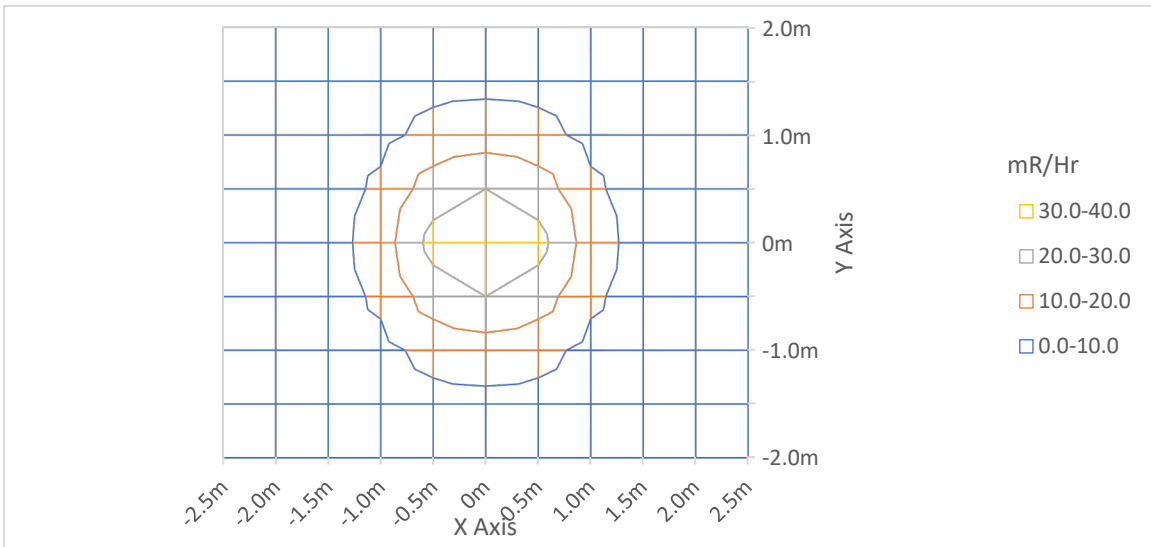


Figure 12: Scatter Exposure Rate Heat Map for 50 kV at Z=75cm

The scatter exposure rate data measured for 50 kV at a plane 25 cm and 75 cm above the SWP plane is shown in Figure 11 & Figure 12. Data obtained for one quadrant has been extrapolated to 360° with the x-ray applicator at the origin for visualization purposes. The highest measured exposure rate was at 0.5 m from the applicator and was measured to be 76.8

mR/hr for detector at 25 cm above SWP and 33.6 mR/hr at 75 cm above the SWP. The exposure rates declined more rapidly for the plane at 25 cm compared to those for at 75 cm above the SWP, as expected. This can be also observed by comparing the slopes of the surfaces in Figures 7 & 8.

Measurements at 1m along the X and Y axis for Z=25 cm plane were 8.9 mR/hr and 12.7 mR/hr, respectively. Measurements at the same locations for Z=75 cm plane were 14.9 mR/hr and 15.1 mR/hr, respectively. This was an unexpected result since the measurements closer to the applicator (at Z=25 cm) were expected to be higher than the measurements that were taken further (at Z=75 cm). A similar trend was observed for the remaining grid points on the XY plane. These differences in scatter measurements indicated that scattered x-rays did not have a point source behavior.

Figure 13 & Figure 14 show the scatter exposure rate data for 70 kV x-ray incident on the SWP at 25 cm and 75 cm above the SWP plane, respectively. Highest measured rates were at 0.5 m from the x-ray tube and were 192 mR/hr at Z=25 cm, and 96 mR/hr at Z=75 cm above SWP, respectively. For grid points at 1m and further from the x-ray tube in the XY plane, the exposure rates for detector 75 cm above SWP plane were greater than those measured at 25 cm above the SWP. This profile of scatter exposure rates for 70 kV was similar to that observed for the 50 kV x-rays.

A similar trend was observed for 100 kV x-ray beam, as shown in Figure 15 & Figure 16. Highest measured rates at 0.5m were 389 mR/hr for detector at 25 cm above SWP, and 194 mR/hr for detector at 75 cm above SWP plane. The decline in exposure rates at 1m and beyond along the XY plane followed the same trend as for 50, and 70 kV, with measurements for grid points at SWP 75 cm above being greater than those for at 25 cm above the SWP plane.

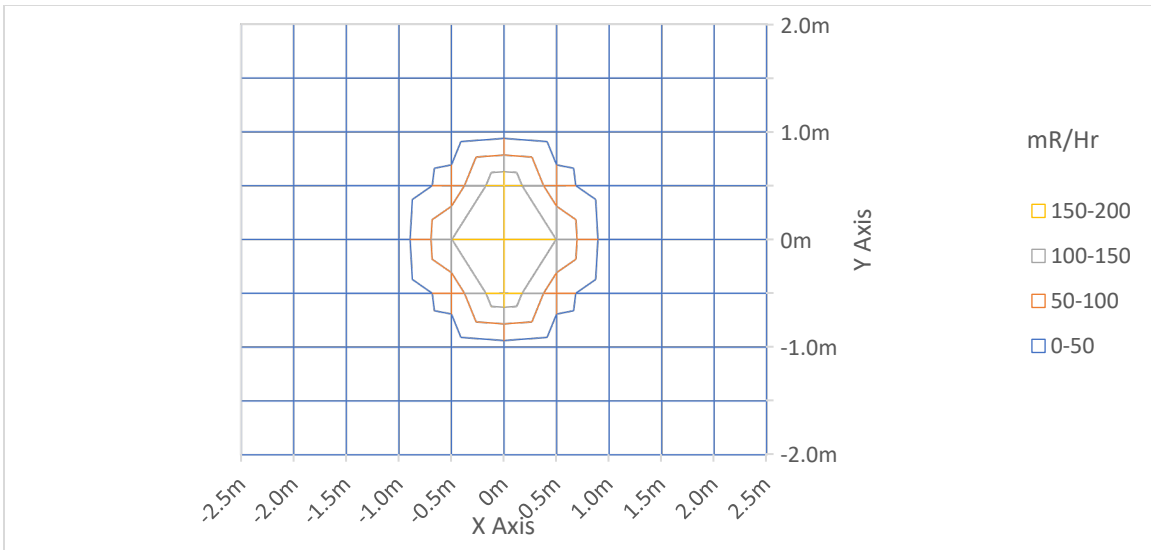


Figure 13: Scatter Heat Map for 70kV at Z=25cm

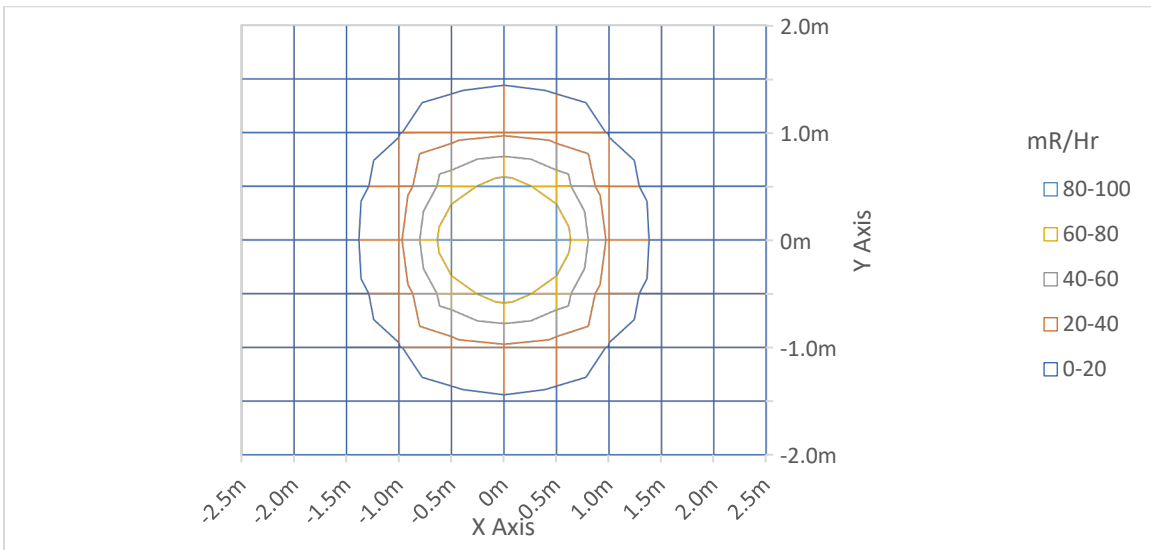


Figure 14: Scatter Heat Map for 70 kV at Z=75cm

The scatter exposure rate profile along the X Axis for 50, 70, and 100 kV are shown in Figure 18, Figure 20, & Figure 22. As discussed earlier, the exposure rate values for measurement at 0.5m from origin is greater for Z=25 cm than Z = 75 cm for all x-ray energies (50, 70, and 100 kV).

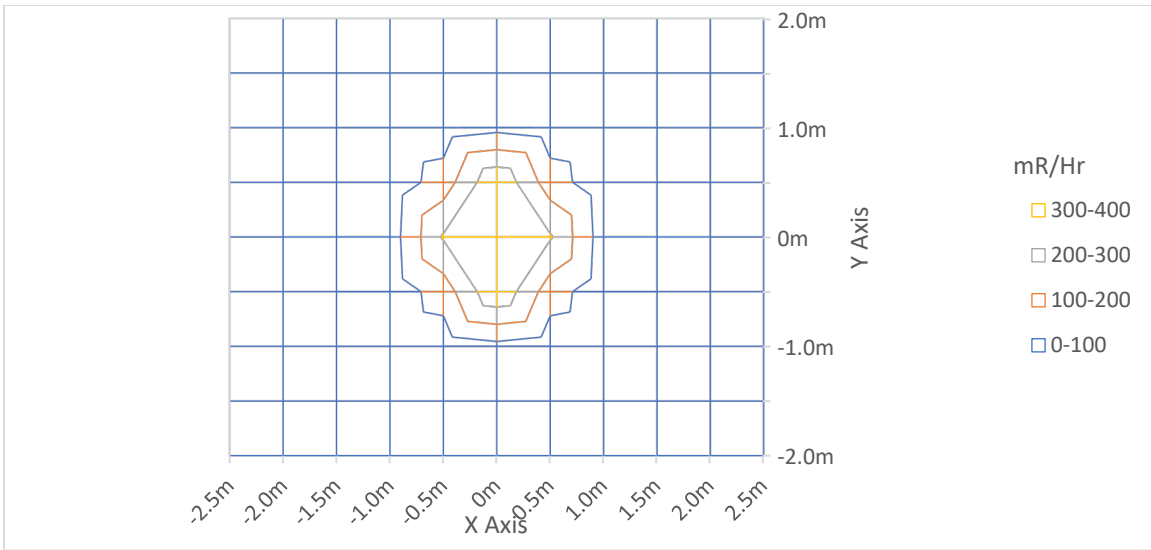


Figure 15: Scatter Exposure Rate Heat Map for 100 kV at Z=25cm

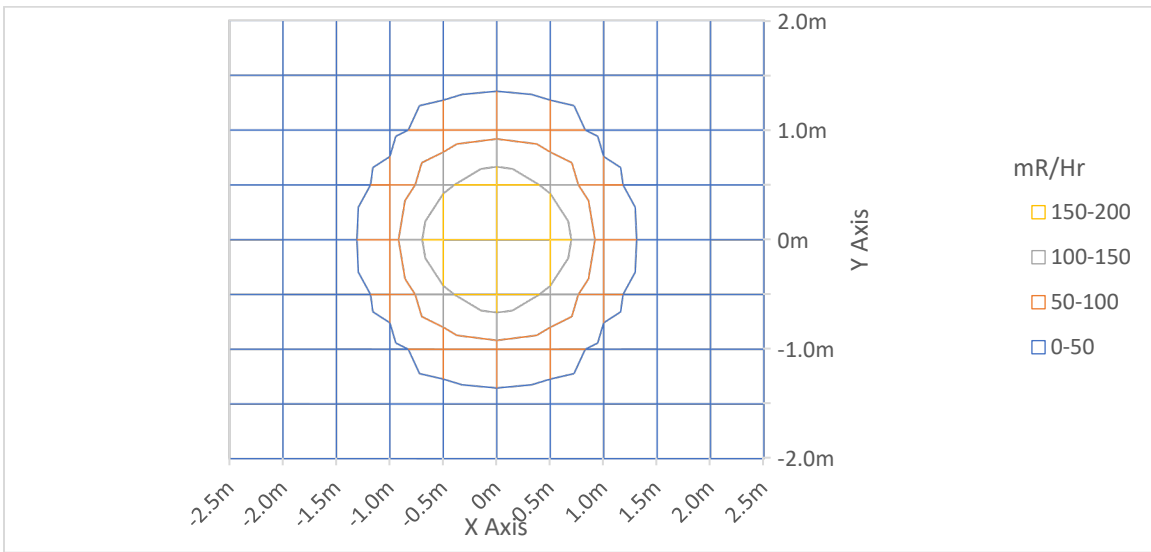


Figure 16: Scatter Exposure Rate Heat Map for 100 kV at Z=75cm

However, at distances greater than 1m, the exposure rate measurements for Z=75 cm is greater than those for Z =25 cm (Figures 18 through 23). There are three possible explanations for this observation a) the detector at 0.5 m and 75 cm above SWP plane is in the shadow of the x-ray tube that is giving an erroneously low exposure rate measurement, b) there is a significant

backscatter from the LINAC table, or c) scatter x-ray from the SWP block do not have an isotropic origin and have an angular component to it.

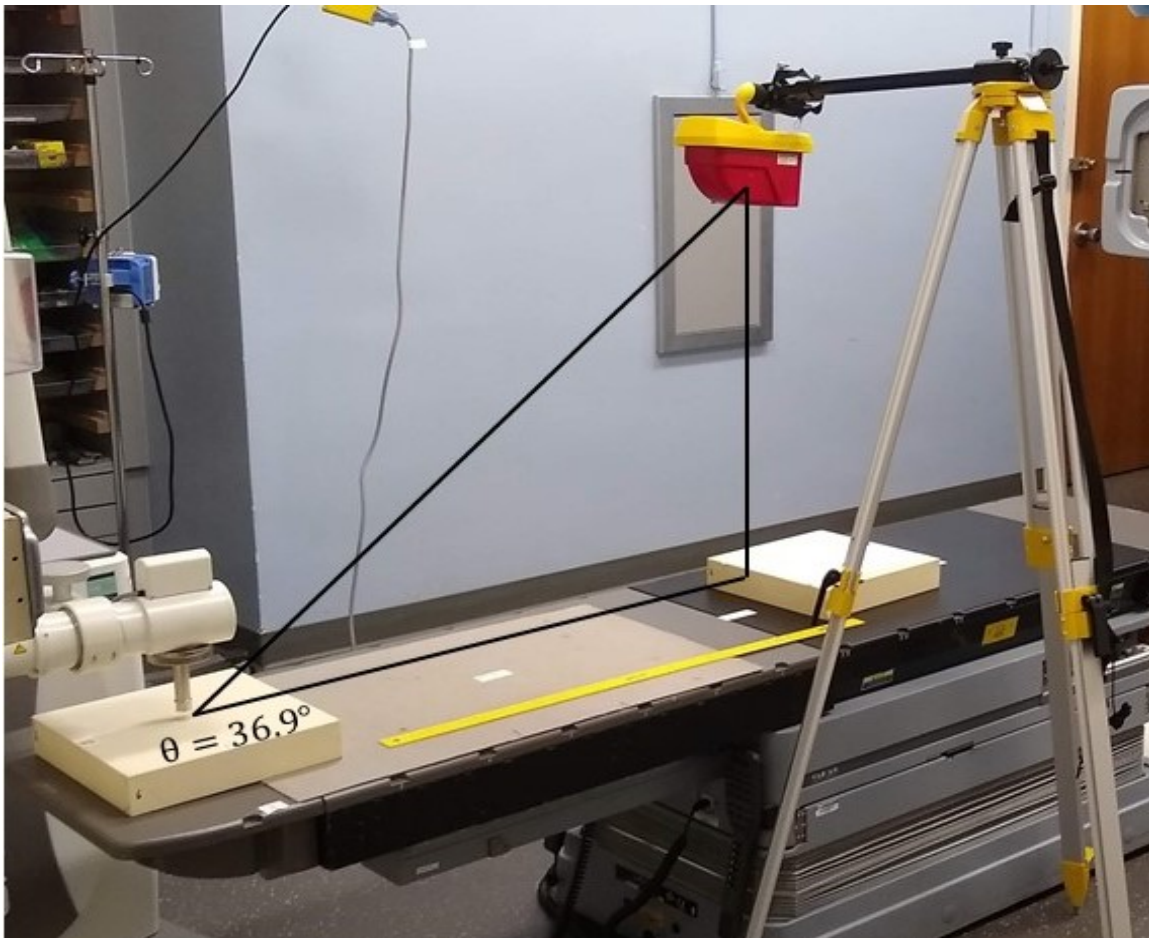


Figure 17: Calculation of Angle Subtended at Applicator by Detector

Figure 17 shows the schematic diagram to calculate the angle subtended by the detector at the applicator tip at the face of SWP. The angle subtended is calculated as shown in Equation (1).

$$\tan^{-1}(\theta) = \frac{\text{distance between detector and SWP plane along Z axis}}{\text{distance between detector and applicator tip along X axis}} \quad (1)$$

$$\tan^{-1}(\theta) = \frac{75 \text{ cm}}{100 \text{ cm}} = 0.75$$

$$\theta = 36.9^\circ$$

Similarly, the angle subtended by the detector at X=0.5m and Z=0.75m is calculated to be 56.3°. Since x-ray tube housing's angle to the applicator tip is greater than 60°, shadowing of scatter x-ray by tube housing is ruled out as possible explanation for this behavior.

Figure 18 through Figure 23 show the exposure rates along the X axis (in this convention, parallel to the LINAC table) and along the Y axis (perpendicular to the LINAC table). Exposure rates along both axes profile exhibit the similar pattern, thus ruling out any significant backscatter contribution from the LINAC table. The hypothesis of an angular component to the backscatter was investigated further in the next experiment.

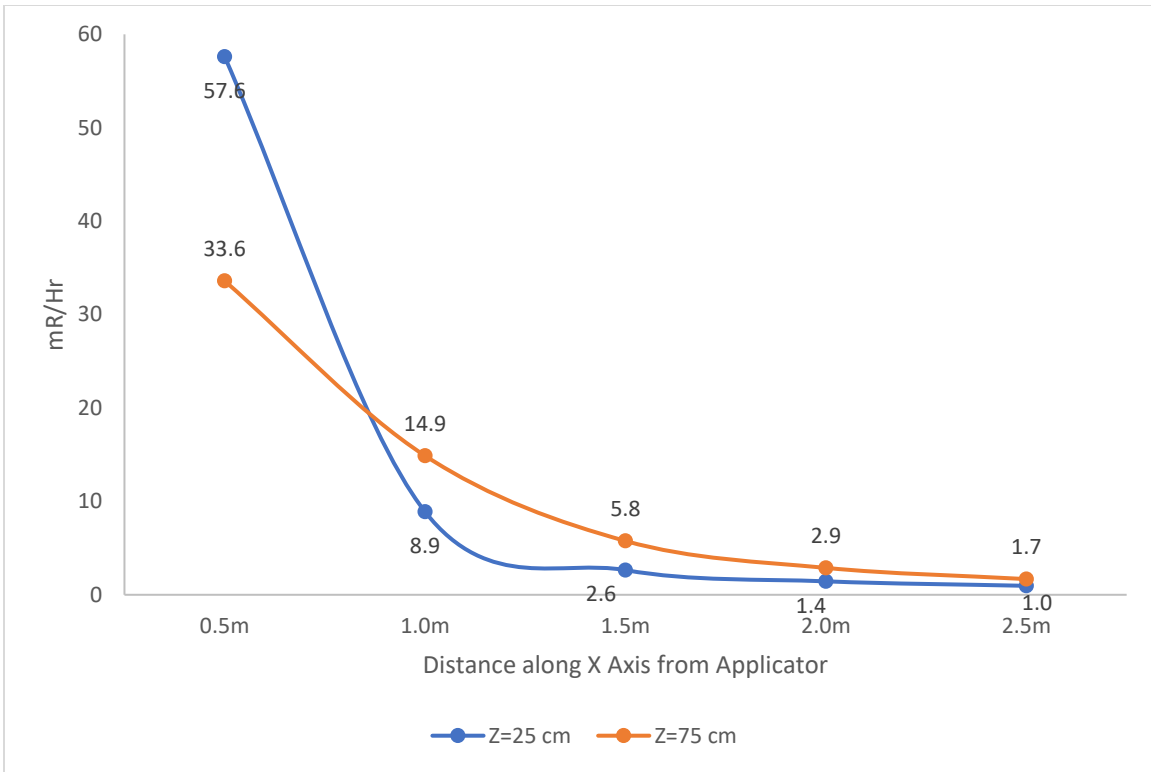


Figure 18: Scatter Exposure Rate Profile for 50 kV x-rays along X Axis

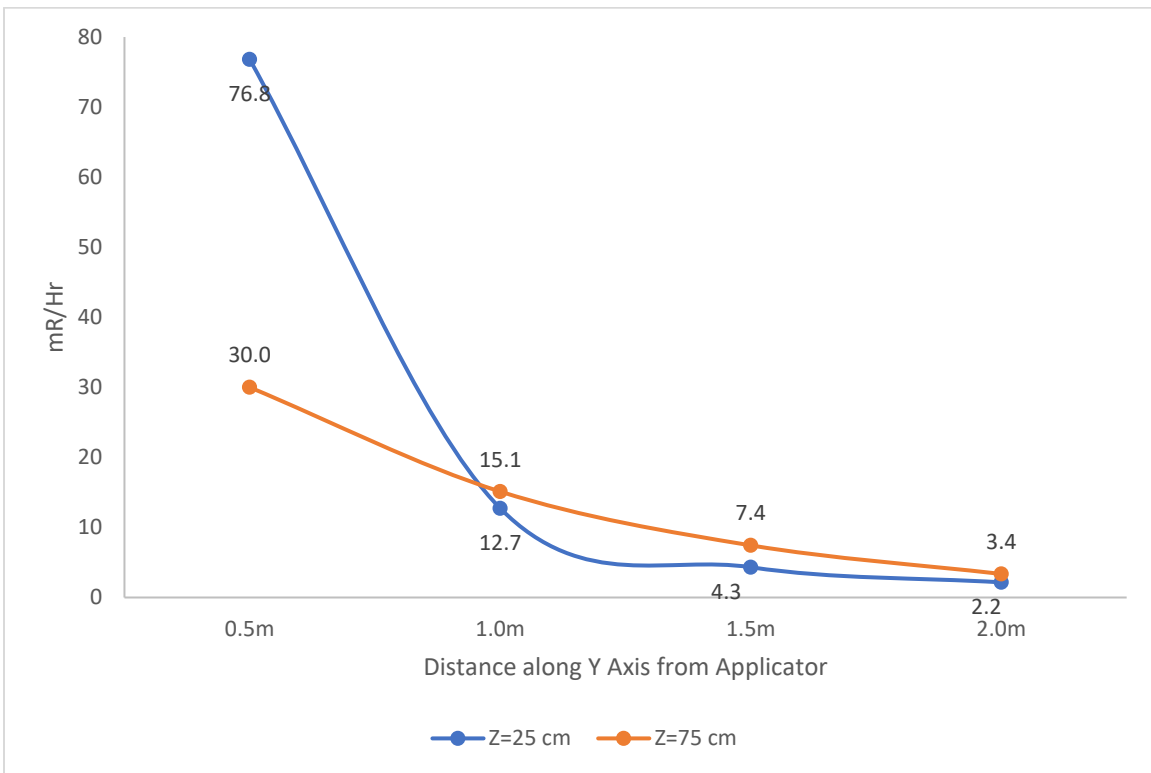


Figure 19: Scatter Exposure Rate Profile for 50 kV x-rays along Y Axis

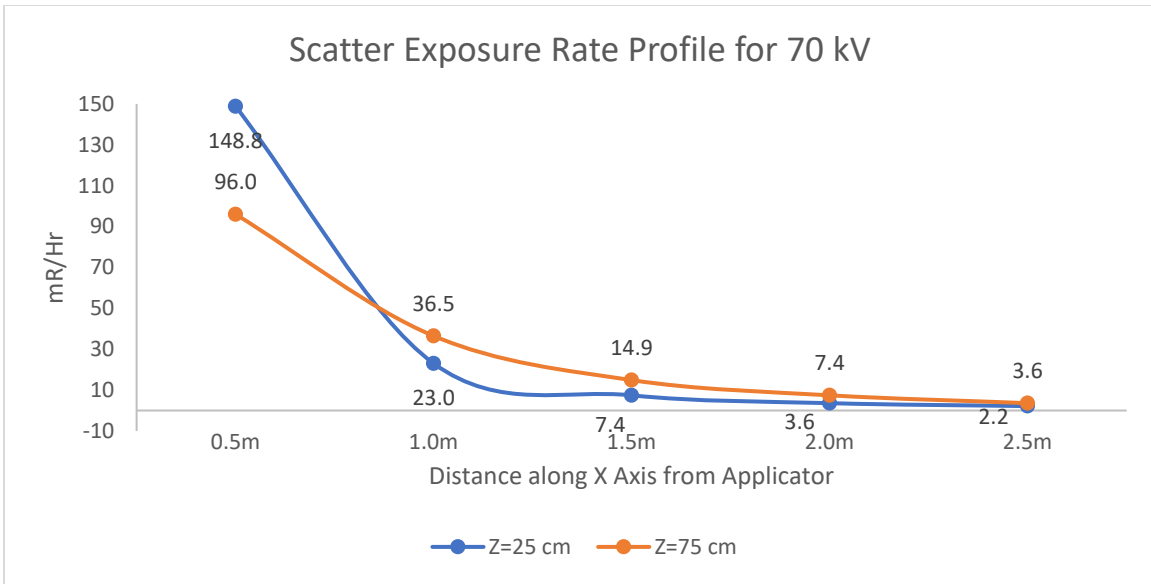


Figure 20: Scatter Exposure Rate Profile for 70 kV x-rays along X Axis

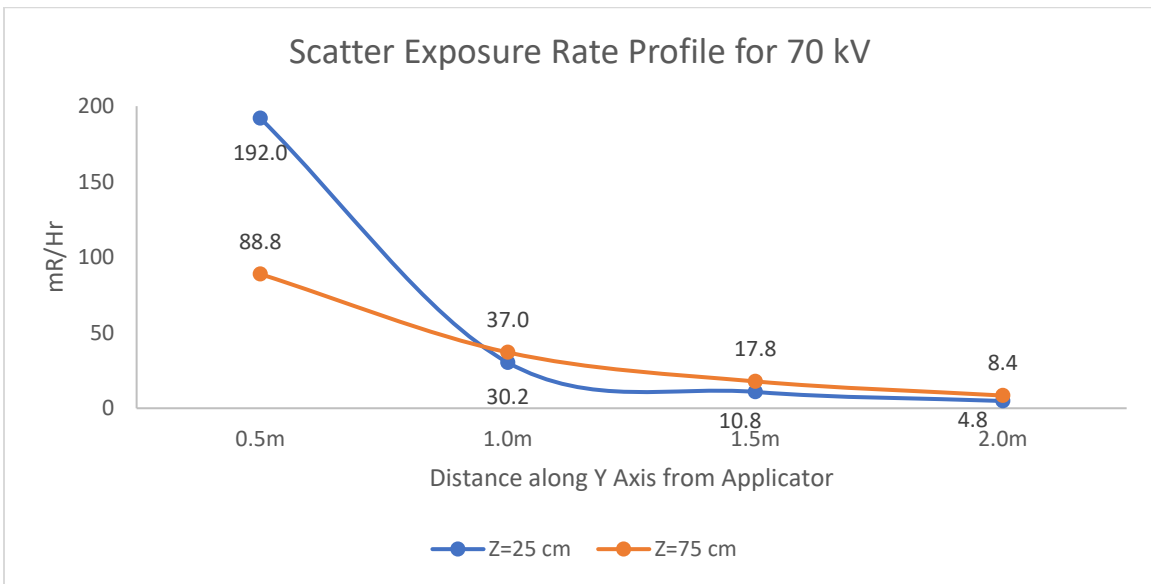


Figure 21: Scatter Exposure Rate Profile for 70 kV x-rays along Y Axis

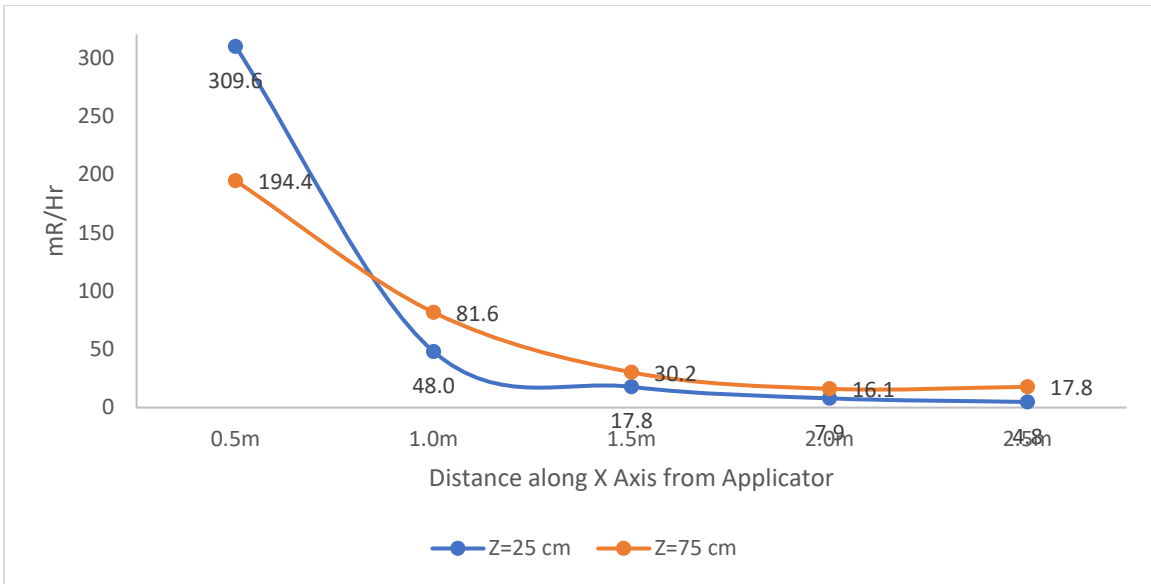


Figure 22: Scatter Exposure Rate Profile for 100 kV x-rays along X Axis

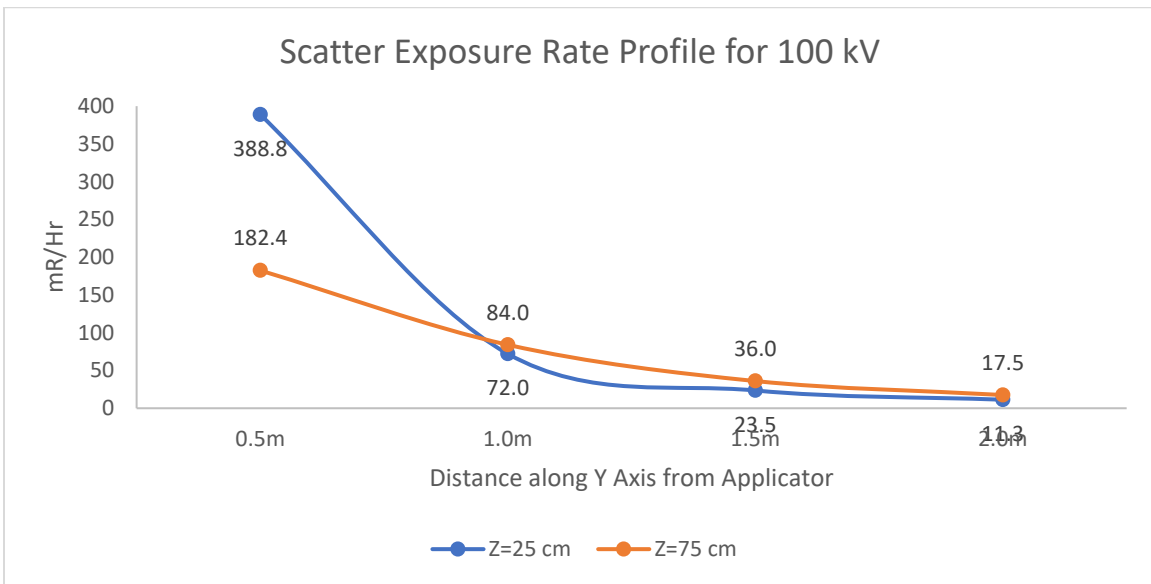


Figure 23: Scatter Exposure Rate Profile for 100 kV x-rays along Y Axis

## Horse Phantom Backscatter

A horse head phantom was utilized to conduct the backscatter experiment for 50, 70, and 100 kV incident beam energy on the phantom's eye. In order to study the angular response of the scatter radiation, from an irregular surface that is typical of a patient's surface, measurements were taken at 0.5m and 1m from the applicator tip, and at angles of 0°, 30°, and 60° to the normal of the applicator axis. Applicator # 4, with a diameter of 2 cm was used for this experiment. The experiment layout is shown in Figure 24. Measurements were taken at the eye level of the horse phantom. Exposure time for the experiment was 15 seconds each and the exposure rates were converted into mR/hr for analysis.

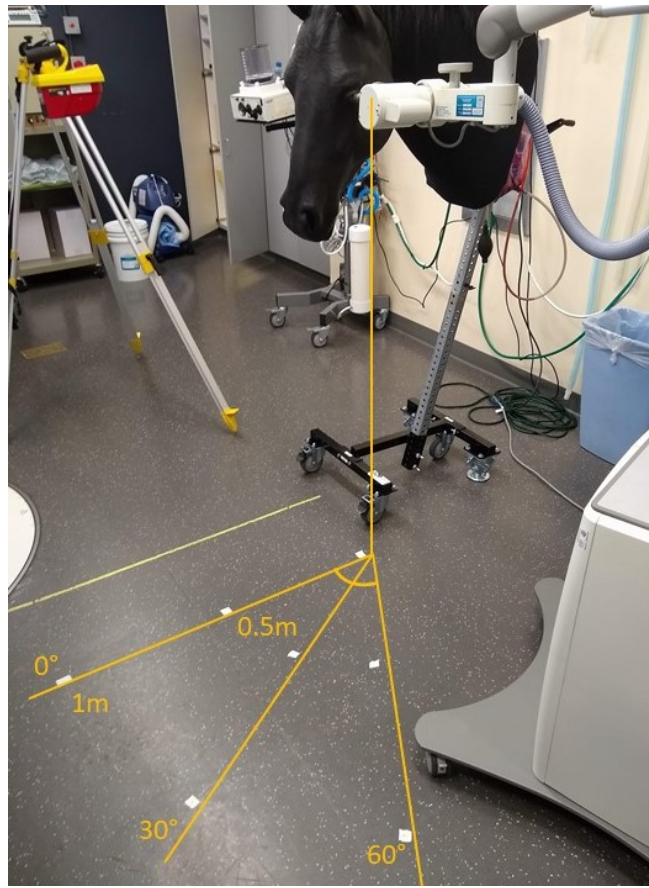


Figure 24: Horse Phantom Backscatter Experiment Layout

The results for this experiment are presented in Figure 25 and Figure 26, for backscatter exposure rates at 0.5m and 1m, respectively. As can be seen from both figures the backscatter exposure rates are lowest at 0° and increase with increasing angles at 30° and 60°.

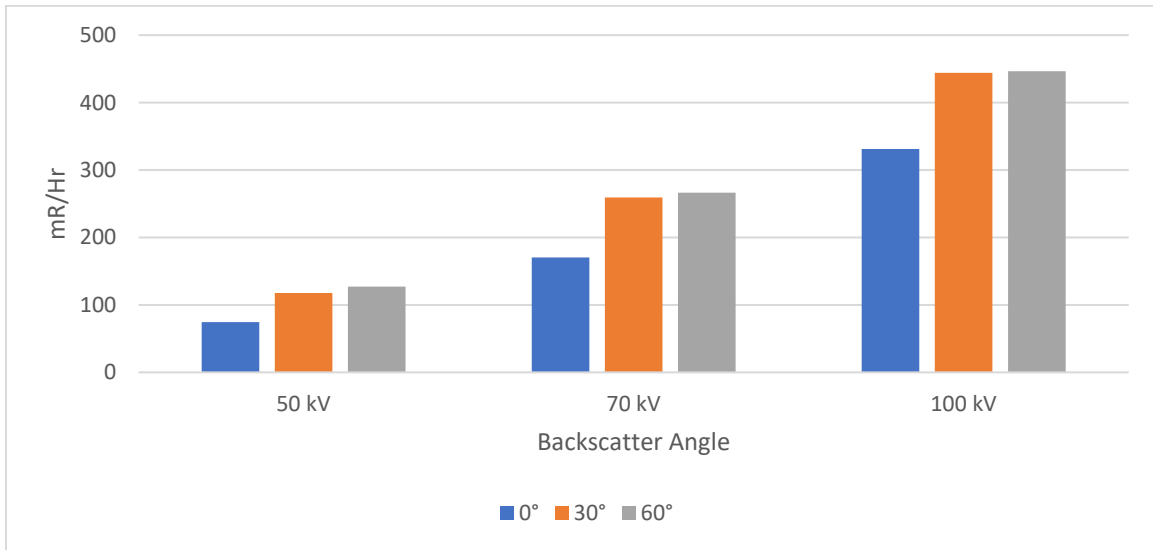


Figure 25: Backscatter Exposure Rates for Horse Phantom at 0.5m

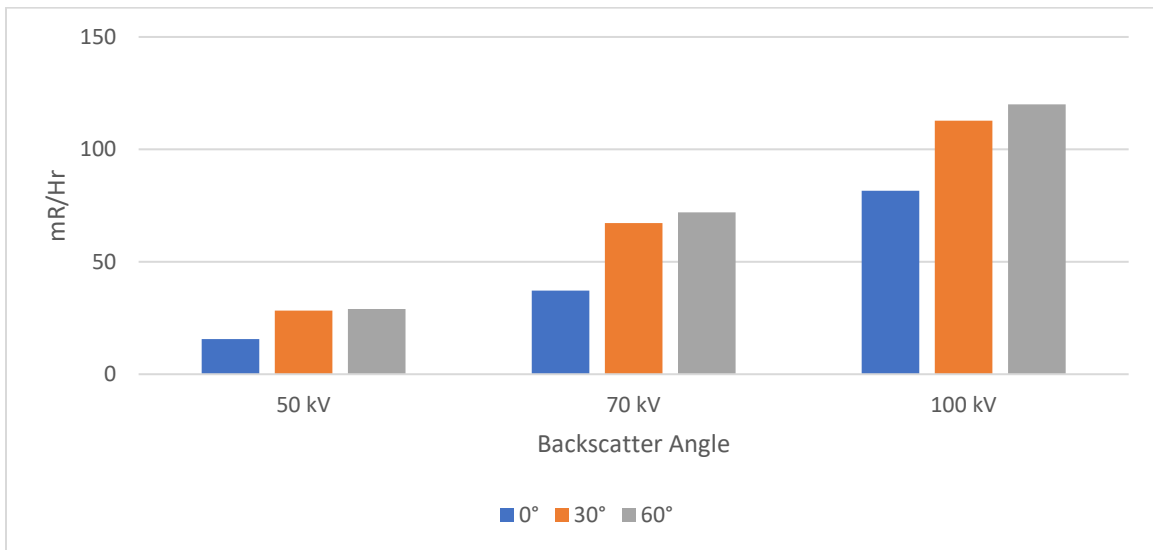


Figure 26: Backscatter Exposure Rates for Horse Phantom at 1m

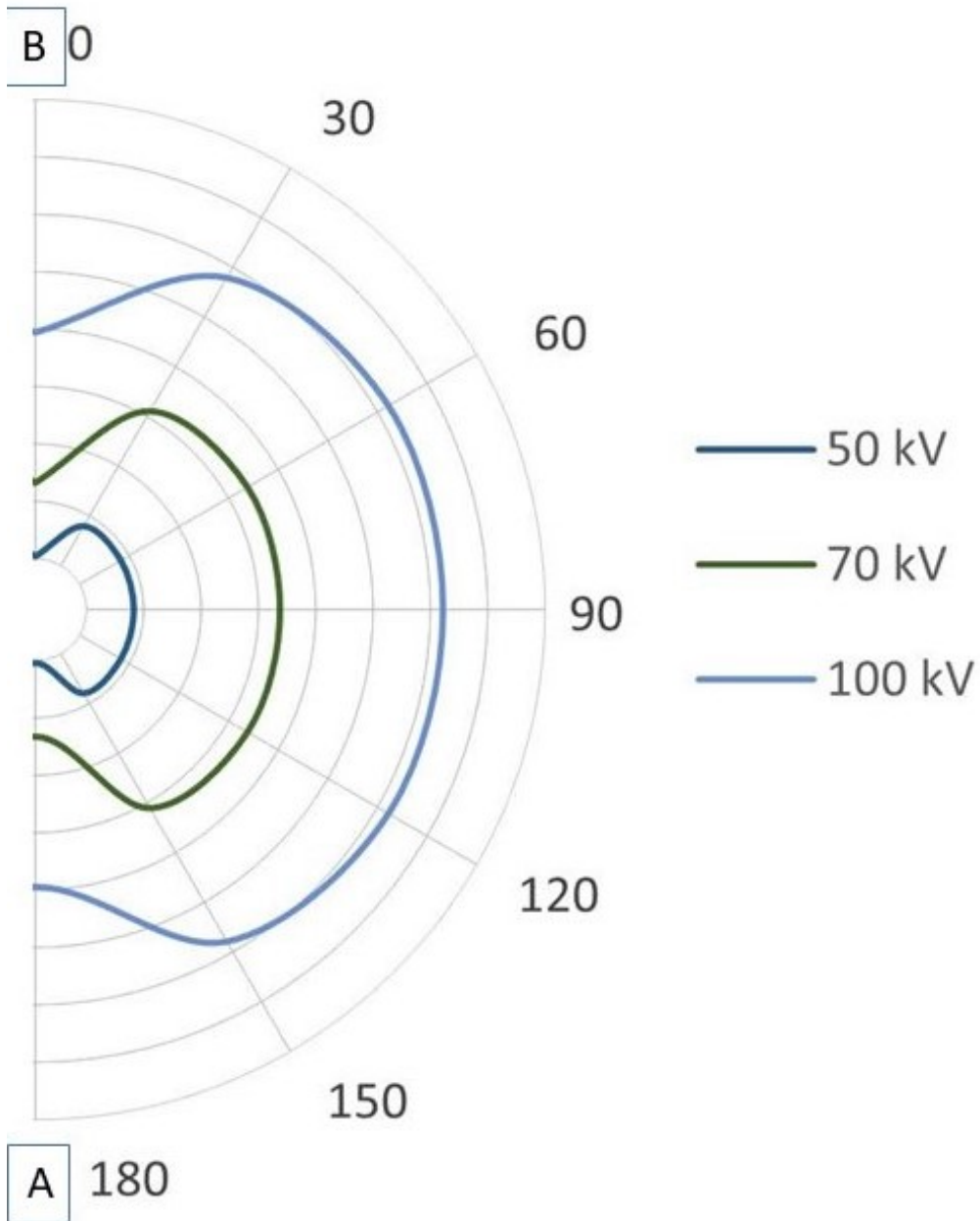


Figure 27: Backscatter Profile for the Horse Phantom at 1m

Figure 27 provides a visual representation of the backscatter profile of the horse phantom, when the phantom is lined along the azimuth angle  $0^\circ$  to  $180^\circ$  tail to head, and the SRT-100 applicator is at  $90^\circ$ . Backscattering of incident x-ray depends on many factors such as energy of the x-ray and the type of material. For organic materials and other low  $Z$  materials, the

backscattering is maximized for x-ray energies less than 100 kV, and for energies in the range of 100-200 kV, high Z materials produce more backscattering radiation than organic material (Huang, Wang, Chen, Xu, & Baozhong, 2018).

The backscatter profile shown Figure 26 is important for finding the optimal location of a veterinary staff when they need to be present in the room during the SRT procedure. Any staff present during treatment should be positioned at location A or B as shown in Figure 27 in order to minimize the backscatter exposure. This backscatter profile also explains the exposure rates in the heat map experiment where higher measurements were observed at Z=75cm compared to Z=25cm at distances greater than 1m.

#### Percentage Depth Dose Curves

Experiments were conducted to generate the percentage depth-dose curves using a Gafchromic film in solid water phantoms for 50, 70, and 100 kV x-rays and for 1.5, 2.0, 2.5, 3.0, and 5.0 cm diameter applicators. EBT3 film was used for this experiment was sandwiched between 2 SWP blocks 6 cm thick as shown in Figure 28. Exposure time for all applicators and x-ray energies was 1 min.

Before generating the PDD, calibration curves for 50, 70, and 100 kV were generated for the batch of EBT3 film to be used as suggested by the manufacturer. The dose delivered to film was controlled by the exposure time for the beam, which ranged from 0.03-3.00 mins for 50 kV, 0.03-2.74 min for 70 kV, and 0.03-1.84 min for 100 kV. Total dose delivered was calculated using equation (2):

$$\text{Dose (Gy)} = \text{Dose Rate for } \times \text{Ray energy } \left( \frac{\text{Gy}}{\text{min}} \right) \times \text{Exposure Time (min)} \quad (2)$$

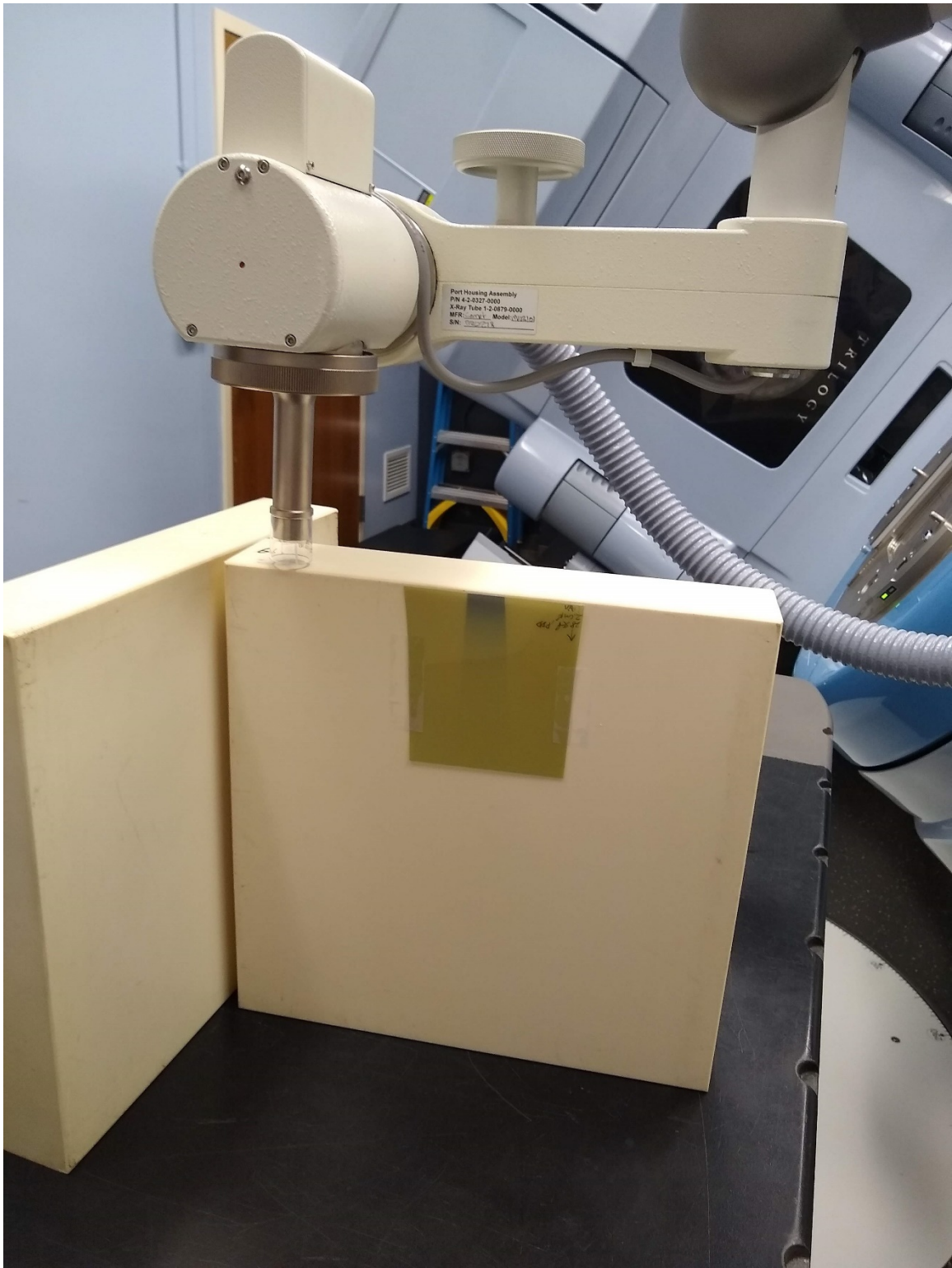


Figure 28: Percentage Depth-Dose Curve Generation Experiment

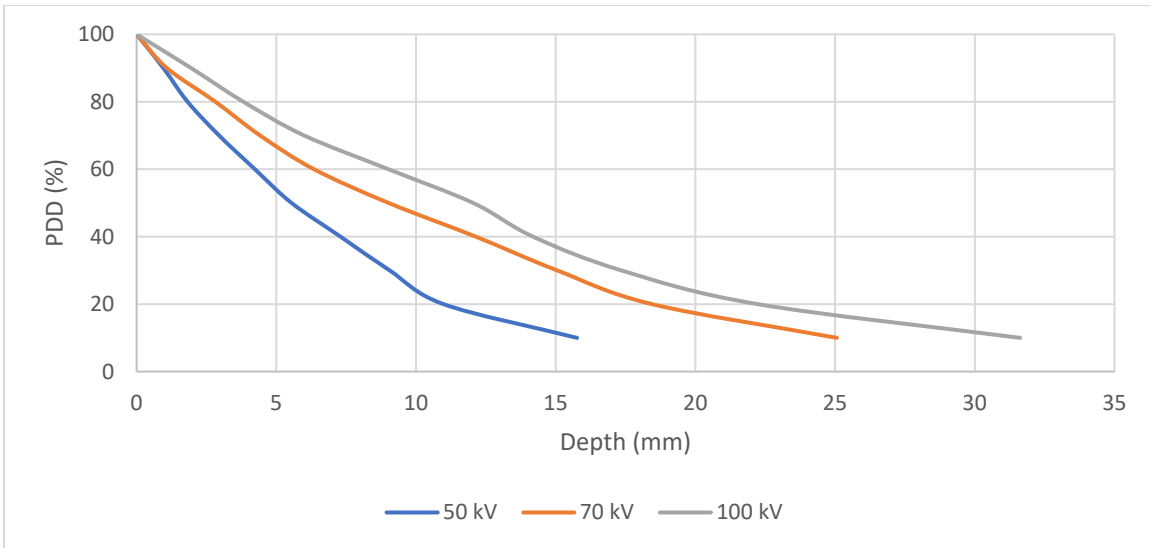


Figure 29: Percentage Depth-Dose Curve for 1.5 cm Applicator

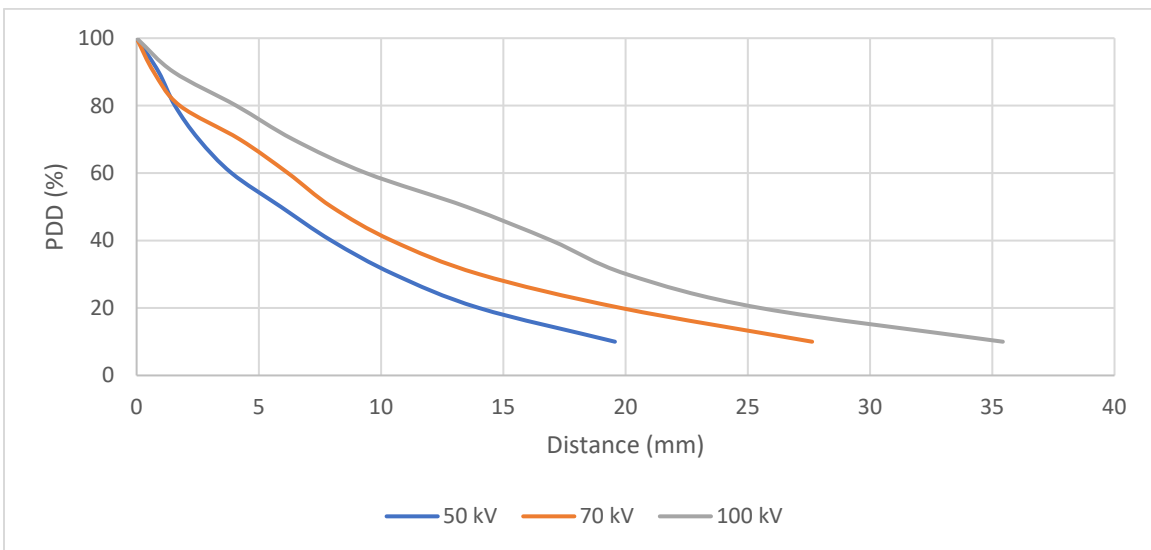


Figure 30: Percentage Depth-Dose Curve for 2.0 cm Applicator

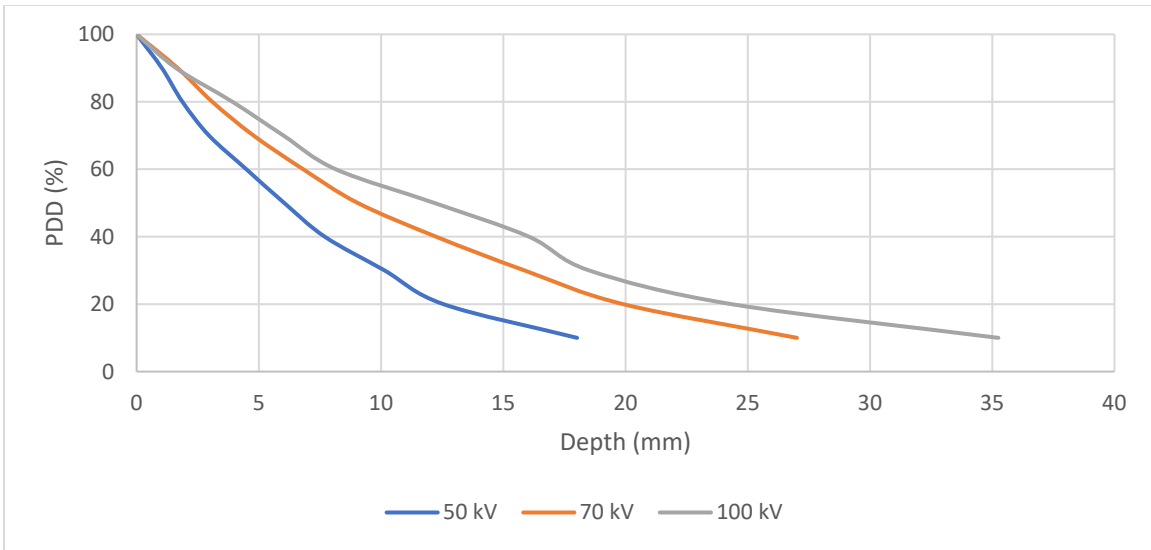


Figure 31: Percentage Depth-Dose Curve for 2.5 cm Applicator

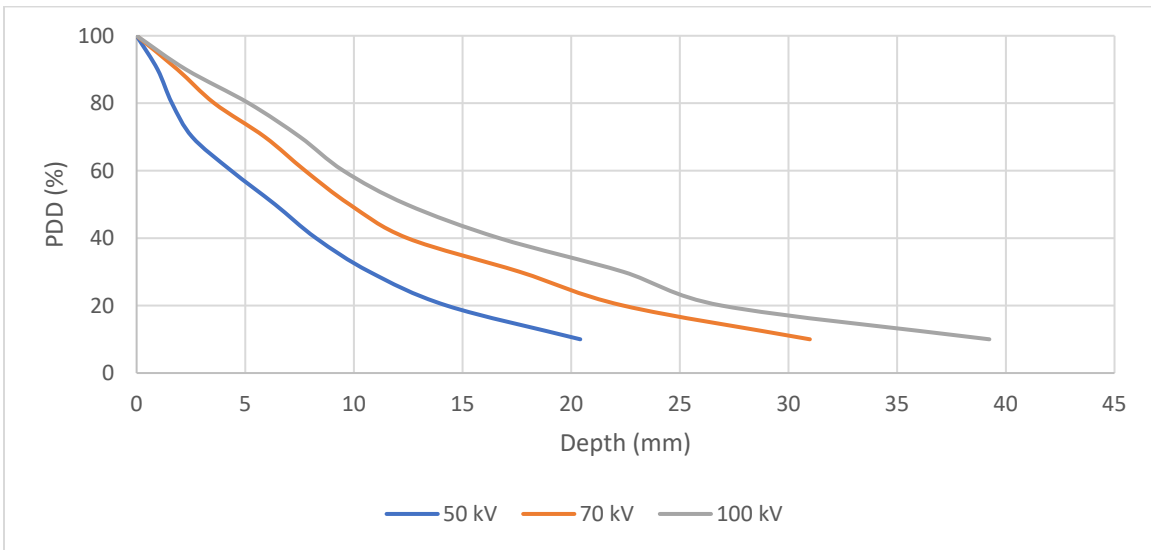


Figure 32: Percentage Depth-Dose Curve for 3.0 cm Applicator

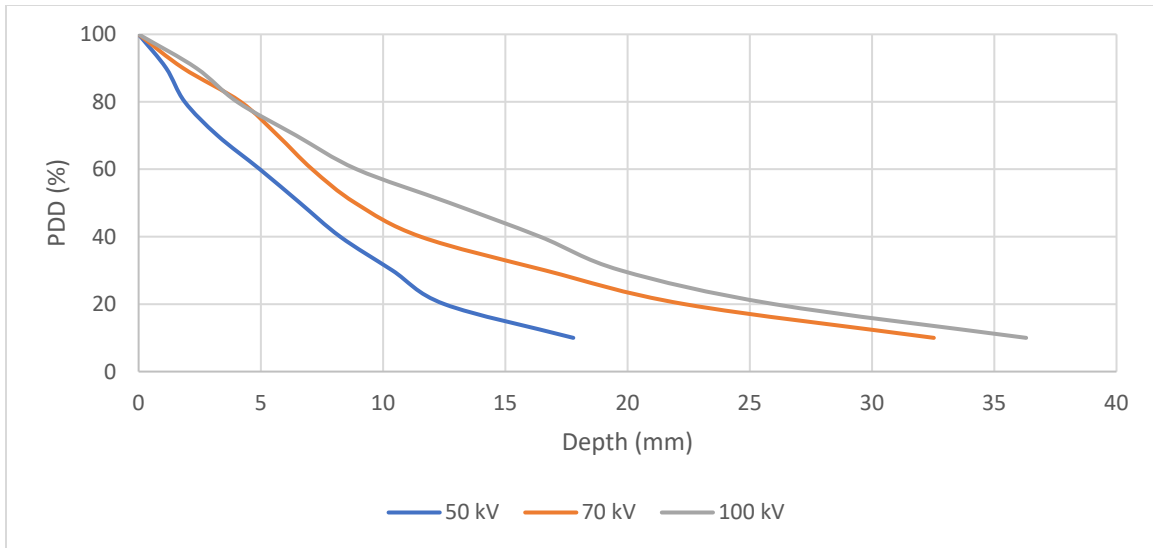


Figure 33: Percentage Depth-Dose Curve for 5.0 cm Applicator

The calibration curves and PDD curves were generated using RIT software. Figure 29- 33 show the PDD curves in SWP for various applicators. For all applicators, the x-ray beam energy was the most important factor with the PDD highest for 100 kV and lowest for 50 kV, at every depth. The PDD curves for 70 kV and 100 kV for some applicators had similar values and the graph appeared to overlap near the surface, this can be attributed to higher dose near the surface and the possibility of some gap being introduced as the blocks were not secured to each other with a mechanical device. Similar studies used SWP block with a 0.25 mm dedicated gap for placing the Gafchromic film to ensure no air gap, and had plastic screws to blocks remained in contact throughout the exposure time (Fletcher & Mills, 2008)

The measured PDD values in this study can be compared to other published measurements. For example, PDD measurements for the 2.5 cm applicator (Figure 31) for 50 kV x-ray was 56.3%, and 30.7% at 1.0 cm. Sheu et al. had similar PDD measurements, 52.2% and 33.8%, respectively (Sheu, Powers, & Lo, 2015).

## DISCUSSION

The purpose of this study was to characterize the x-ray scatter, x-ray field, and exposure levels being emitted in the vicinity of the SRT-100™ unit. This was done in order to explore the safety of personnel near large animal patients undergoing radiation treatment of superficial skin conditions. X-ray exposure measurements were acquired around the x-ray unit at various locations and under various treatment conditions to characterize the scatter field that may be in excess of personnel exposure limits. In addition, the optimal location for personnel to be positioned during SRT was identified where dose due to the scattered x-rays would be minimized.

### Detector Orientation Dependence

Detector orientation with respect to the x-ray tube location results in a variation in the measured exposure rates. The normalized angular response when detector was rotated vertically from 0° to 90° ranged from 94.1% to 103.9% (50 kV), as shown in Table 2. Similarly, the response when detector was rotated horizontally ranged from 90.9% to 109.4% (Table 3). With these data, the detector orientation was kept nearly constant to minimize the angular response of the detector.

### Exposure with Varying Energy and Applicator Size

The SRT-100 system is fairly simple to use and has two critical planning factors, the energy of x-ray being produced and the applicator size. Our system consisted of Nine different applicators and three x-ray beam energies; these were studied in combination to determine

scatter radiation doses to operators. The exposure rates measured at the surface of SWP blocks increased significantly as the cross sectional area of the applicator increased. Knowledge of exposure rates in the vicinity of SRT is important for radiation safety as bigger applicators mean more dose to the patient and more scatter radiation emission. However, surrounding exposure due to x-ray beam energy was much more pronounced than applicator size, as exposure rates increased by more than one order of magnitude between 50 kV and 100 kV for some applicators.

An exposure heat map was generated in the vicinity of the applicator to visualize the levels of scatter x-ray being emitted. As expected, scatter exposure rates increased with increasing the x-ray beam energy, with 100 kV providing the highest exposure rates around the machine. Measurements at 0.5m had highest exposure rates, with measurements at 25 cm above the SWP plane greater than those measured at 75 cm above the SWP plane. However, for measurements at grid points farther than 1m from applicator the exposure rates at 25 cm above the SWP plane were lower than those measured at 75 cm above the SWP plane. This anomalous trend was observed for all x-ray beam energies (Figures 18, 20, & 22).

Possible explanations for this result were shadow effect of x-ray tube for grid point 0.5m and 75 cm above the SWP plane, but that was ruled out based on the observed angle subtended between applicator tip and detector being greater than angle required for a shadow effect by the x-ray tube housing (Figure 17). Additional scattering from the LINAC gantry table was also ruled out as the similar results were observed when measurements were taken along the Y axis, where backscatter from LINAC table was not a factor (Figures 19, 21, & 23). This pointed to an angular component to the scatter x-ray being emitted from the SWP blocks in this experiment with more scattering along the applicator axis that drops at normal angles.

## Exposure and Occupational Time Limits

Exposure data from the Scatter heat map experiment at Z=25 cm along the X axis were used to estimate dose to personnel in the vicinity during the SRT treatment (Table 5). For scatter dose estimates, 1 R of incident x-ray radiation was used as a conservative estimate to deliver 1 rad of dose equivalent in soft tissue (1R=0.95 rad) (Turner, 1995). Occupational Safety and Health Administration (OSHA) limits the whole-body dose received to a radiation worker in one calendar quarter to less than 1¼ rem, as stipulated in 29CFR1910.1096(b)(1).

Table 5: Estimated Dose Rates (mrem/hr) at various distance from applicator

Beam Energy	Estimated dose rate (mrem/hr)				
	0.5m	1.0m	1.5m	2.0m	2.5m
50 kV	57.6	8.88	2.64	1.44	0.96
70 kV	148.8	23.04	7.44	3.6	2.16
100 kV	309.6	48	17.76	7.92	4.8

In keeping with the ALARA principles, 10% of regulatory quarter dose limit (125 mrem) was used as the threshold dose limit to determine the residence time in the room, i.e. the time duration for which personnel can stay in the treatment room without exceeding the 125 mrem/quarter dose limit. The residence time at each distance was calculated using equation (3) and are provided in (Figure 34) for 50, 70, and 100 kV for 0.5m to 2.5m distance from the applicator.

$$\text{Residence time (minutes)} = \frac{10\% \text{ Dose Limit (125 mrem)}}{\text{Dose rate} \left( \frac{\text{mrem}}{\text{hr}} \right)} \times 60 \frac{\text{min}}{\text{hr}} \quad (3)$$

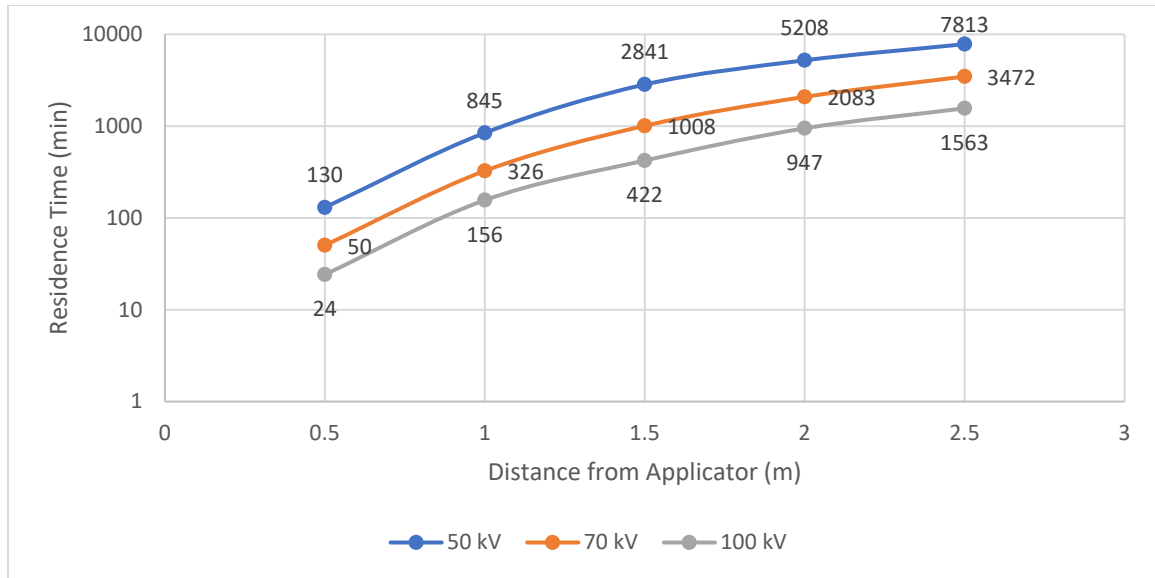


Figure 34: Residence time in treatment room without any PPE

The residence time in Figure 34 are for personnel not using any lead apron as personal protective equipment (PPE). Typically, radiation workers wear a lead apron that has 0.25 mm lead equivalent. HVL for a broad beam x-ray (Turner, 1995), attenuation coefficients, and attenuation by 0.25 mm of lead apron values are given in Table 6.

Table 6: HVL, attenuation coefficients, and attenuation factor broad beam x-ray

Beam Energy	HVL for Lead (mm)	Attenuation Coefficient ( $\text{mm}^{-1}$ )	Attenuation by 0.25 mm Lead apron
50 kV	0.06	11.55	17.96
70 kV	0.17	4.08	2.77
100 kV	0.27	2.57	1.90

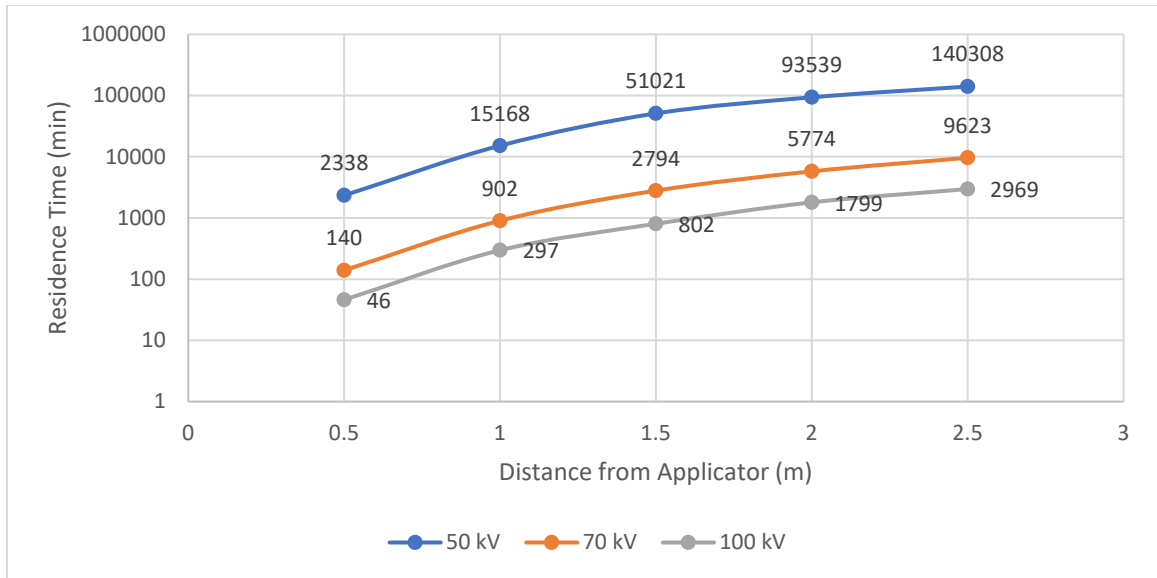


Figure 35: Residence time in treatment room with lead apron

#### Energy Response Correction Factor

The energy response factor for 50, 70, and 100 kV of model 451P ion chamber was found to be 0.4, 0.45, and 0.7, respectively (Anonymous, 2013). This factor was used to calculate the energy corrected residence time shown in Figure 36. Angular dependence data from the horse head phantom experiment was applied to the energy corrected residence time values in Figure 38.

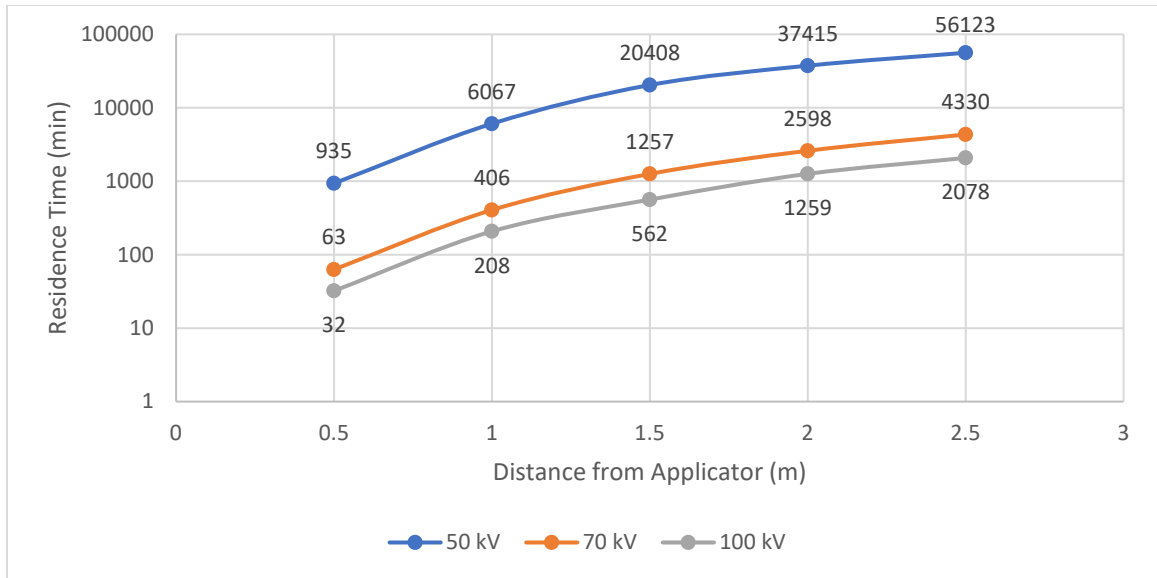


Figure 36: Energy corrected residence time in treatment room with lead apron

#### Angular Scattering from Horse Head Phantom

Based on the angular dependence data, the optimal location for veterinary personnel to be positioned during the SRT in order to minimize dose from scatter x-rays will be at location A as shown in Figure 37, which corresponds to  $0^\circ$  in Figure 38: Angular dependence of residence time at 1 m. Personnel positioned around the horse at location B, which corresponds to  $60^\circ$  in Figure 38 will receive a comparatively higher dose because of greater x-ray scattering from the horse head. Note that Figure 38 is residence time where higher values indicate lower exposure rates.



Figure 37: Optimal Location for Veterinary Personnel during SRT

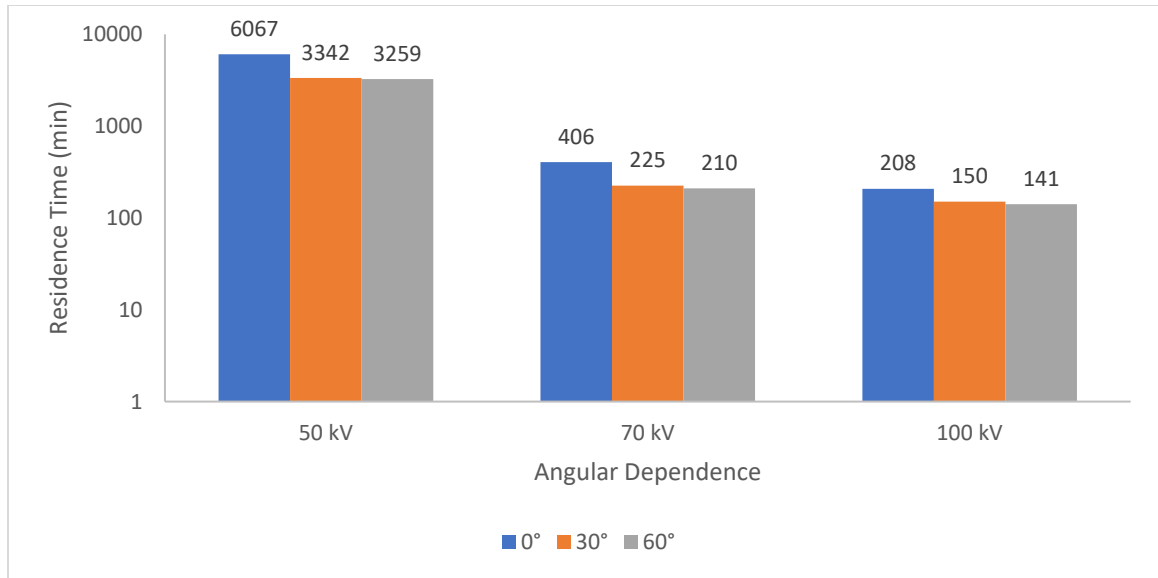


Figure 38: Angular dependence of residence time at 1 m

An estimate of distances at which dose rate is below 2 mrem/hr was calculated based on the dose rate data at  $Z = 25$  cm for 50, 70, and 100 kV beam energies measured along the X axis (Figures 18, 20, & 22). The 2 mrem/hr dose rate limit was determined by fitting a function using these data and extrapolating to the threshold limit (Figure 39, 40, & 41). The equations of best fit were determined and the distance from applicator at which dose rate is 2 mrem/hr was calculate for each beam energy and is shown in Figure 42.

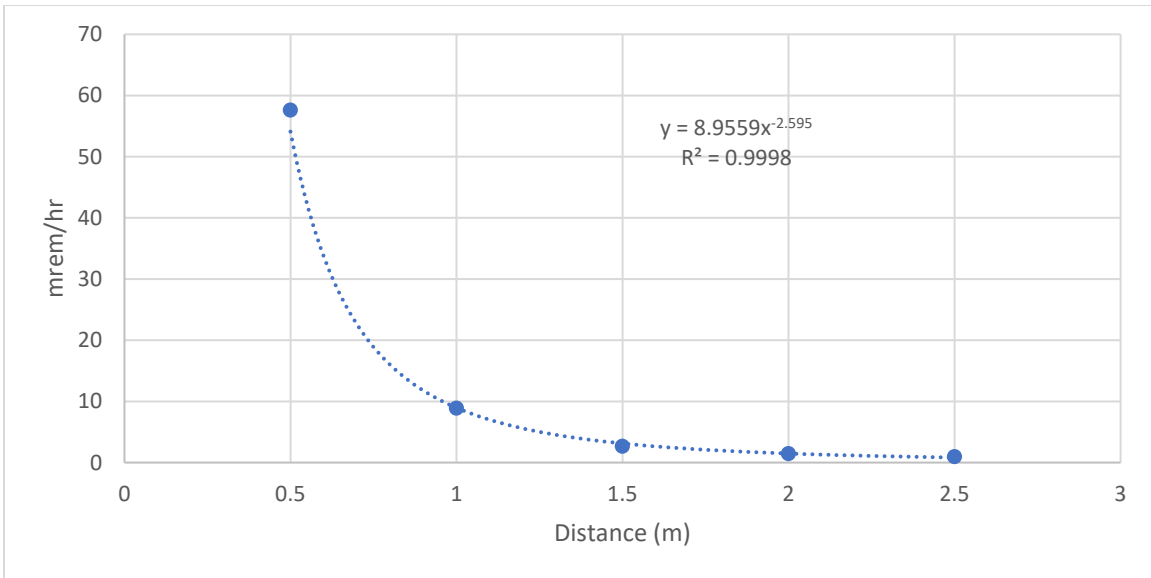


Figure 39: Dose Rate vs Distance for 50 kV

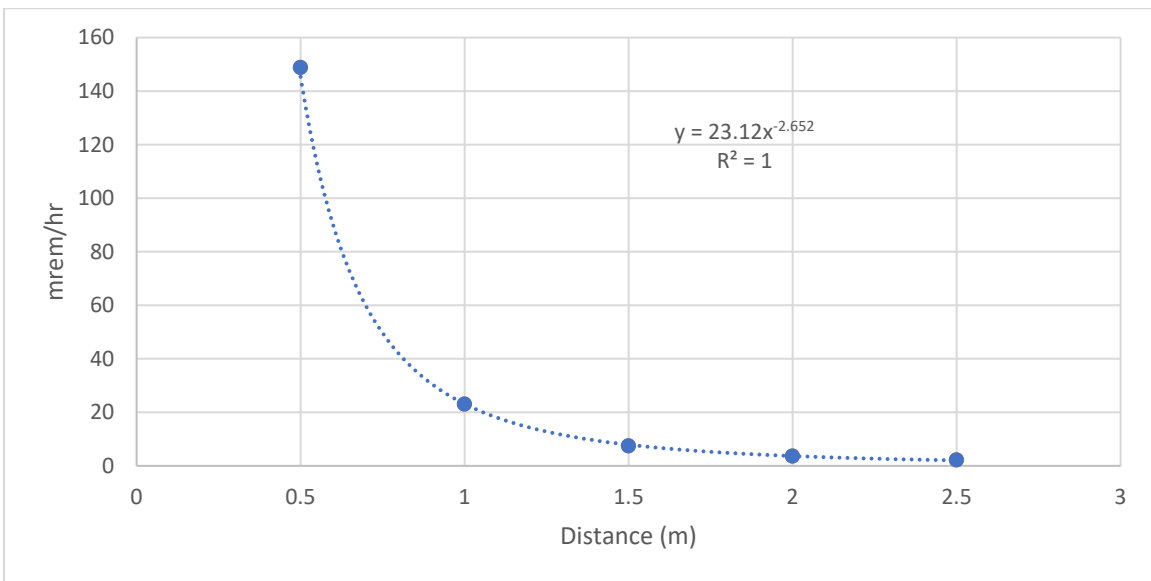


Figure 40: Dose Rate vs Distance for 70 kV

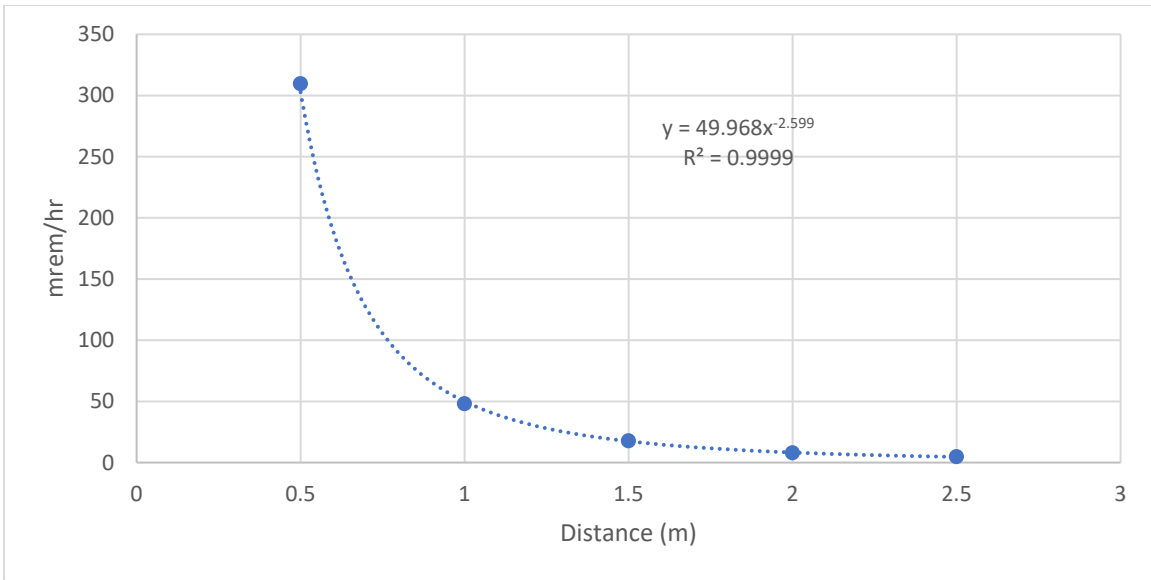


Figure 41: Dose Rate vs Distance for 100 kV

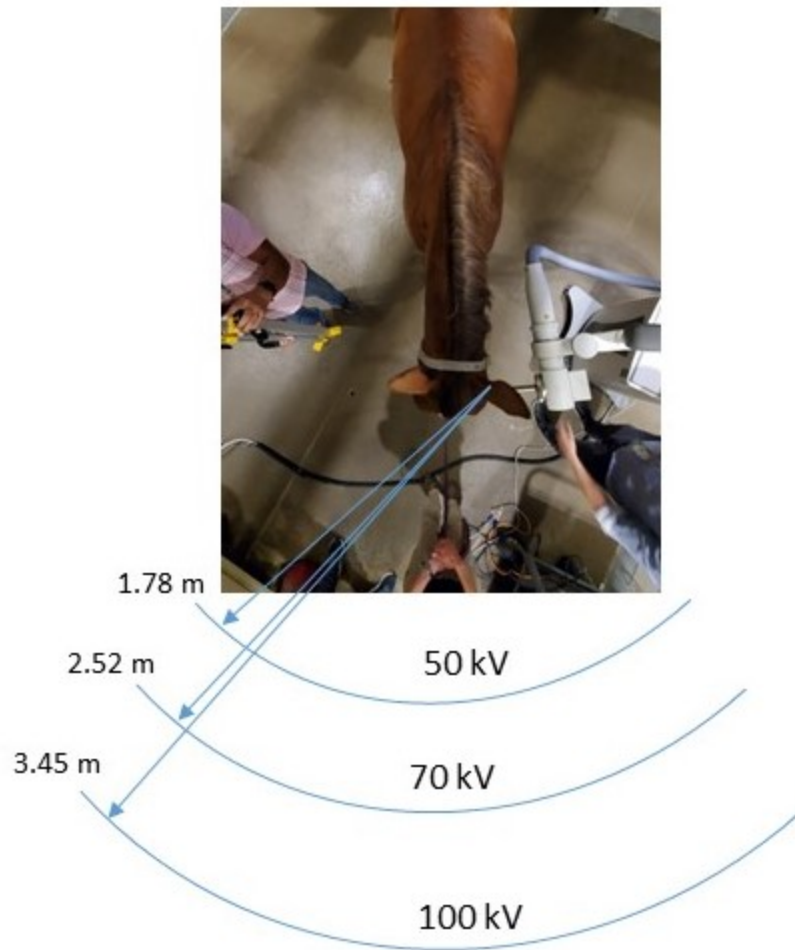


Figure 42: Estimated Distance from Applicator for 2 mR/hr Exposure Rate

PDD curves were generated for 5 applicators for 50, 70, and 100 kV x-rays. As expected, PDD values for 100 kV x-rays were significantly higher for a given depth, than those for 50 and 70 kV (Figures 29-33). The vertical profile for all measurements did follow the decrease in dose with depth as has been reported in literature. However, the PDD measurements obtained during this study at various depths were different from those that had been reported by the manufacturer and reported in other studies. The primary reason for this would be the difference in the inherent beam filtration for various x-ray tubes leading to beam hardening. The HVL (Al equivalent) for SRT-100™ used for this study was 0.43 mm and has been reported as high as 0.53 - Similarly for 70 kV the HVL was 1.04 mm and is reported to be 1.15 mm, and for 100 kV the HVL was 1.87 mm and is reported to be 2.10 mm in similar studies (Sheu, Powers, & Lo, 2015). The difference in x-ray filtration will affect the PDD values and make a direct comparison difficult between the studies.

## CONCLUSIONS

The SRT-100™ Superficial Radiation Therapy system is a viable option for treating skin lesions that cannot be surgically removed in veterinary patients. The SRT presents a radiation exposure challenge for veterinary staff in certain situations. During the SRT treatment, applicator size and x-ray energy were proven to be the critical parameters in the emission of scatter x-rays in the vicinity of the applicator.

Exposure rates were measured at 58 locations around the SRT-100™ applicator to characterize the scatter x-ray being produced during the treatment. There is an angular component to the backscatter from the SWP blocks. An experiment was conducted to study the backscatter from a horse phantom and a profile of scatter x-ray created (Figure 27). Scatter exposure rates were higher along the direction of the applicator tube than compared to the perpendicular direction of the applicator. The exposure rate mapping provided information related to placement of veterinary staff during an SRT procedure in order to minimize their dose from scatter x-ray being produced during treatment.

Based on the scatter x-ray measurements it is concluded that veterinary personnel can be present in the room for the SRT for large animals and are not expected to reach 10% of quarterly dose limits (Figure 34). Estimates of residence time for personnel to reach 10% of quarterly dose limits were made for when personnel wear 0.25 mm lead PPE (Figure 35). Wearing lead PPE during SRT will further reduce the occupational dose for veterinary personnel. An estimate of distance where dose rate from scatter x-ray reduces to 2 mR/hr was performed for 50, 70, and 100 kV (Figure 42).

Available scientific literature was reviewed to evaluate the efficacy and performance of electronic personal dosimeters in order to provide real time dose measurements. A commercially available electronic personal dosimeter was recommended based on its capabilities, to be used in conjunction with the passive dosimeter during the SRT procedures at the veterinary hospital.

Percentage depth-dose curves were generated using EBT-3 Gafchromic film for various x-ray energies and applicators. These curves did exhibit the general behavior as is reported in other studies. However, the PDD values obtained during this experiment were not in agreement with the values provided by the SRT-100™ manufacturer. An estimation of scatter dose emitted during x-ray SRT treatment can be obtained using modeling software like MCNP and compared to measurements obtained using ion chambers with a significantly smaller active volume to provide better spatial resolution in the vicinity of source.

## REFERENCES

- Al-Ghorabie, F. (2015). Experimental measurements and Monte Carlo modelling of the XSTRAHL 150 superficial X-ray therapy unit. *Journal of Radiotherapy in Practice*, 43-55.
- Allgoewer, I., & Hoecht, S. (2010). Radiotherapy for canine chronic superficial keratitis using soft X-rays (15 kV). *Veterinary Ophthalmology*, 20-25.
- Anonymous. (2013). 451P Ion Chamber Survey Meter . *Operators Manual*. Everett, WA, USA: Fluke Biomedical.
- Berman, B., Nestor, M. S., Gold, M. H., Goldberg, D. J., Weiss, E. T., & Raymond, I. (2020). A retrospective registry study evaluating the long-term efficacy and safety of superficial radiation therapy following excision of Keloid scars. *Journal of Clinical and Aesthetic Dermatology*, 12-16.
- Cognetta, A. B., Howard, B. M., Heaton, H. P., Stoddard, E. R., Hong, H. G., & Green, W. (2012). Superficial x-ray in the treatment of basal and squamous cell carcinomas: A viable option in select patients. *Journal of American Academy of Dermatology*, 1235-1241.
- Federal Register. (2020, March 18). Individual Monitoring Devices. *Direct Action Rule*. US Government Publishing Office.
- Fetterly, K. A., Schueler, B. A., Grams, M. P., & Sturchio, G. M. (2017). Estimating head and neck tissue dose from x-ray scatter to physicians performing x-ray guided cardiovascular procedures: a phantom study. *Journal of Radiological Protection*, 43-58.

- Fletcher, C. L., & Mills, J. A. (2008). An assessment of GafChromic film for measuring 50 kV and 100 kV percentage depth dose curves. *Physics in Medicine and Biology*, N209-N218.
- Ginjaurme, M., Bolognese-Milsztajn, T., Luszik-Bhadra, M., Vanhavere, F., Wahl, W., & Weeks, A. (2007). Overview of active personal dosimeters for individual monitoring in the European Union. *Radiation Protection Dosimetry*, 261-266.
- Goldschmidt, H., Breneman, J. C., & Breneman, D. L. (1994). Ionizing radiation therapy in dermatology. *Journal of the American Academy of Dermatology*, 157-182.
- Guo, S., Reddy, C. A., Kolar, M., Woody, N., Mahadevan, A., Deibel, C. F., . . . Suh, J. S. (2012). Intraoperative radiation therapy with the photon radiosurgery system in locally advanced and recurrent rectal cancer: retrospective review of the Cleveland clinic experience. *Radiation Oncology*, 1-8.
- Halpern, J. N. (1997). Radiation therapy in skin cancer A historical perspective and current applications. *Dermatological Surgery*, 1089-1093.
- Huang, S., Wang, X., Chen, Y., Xu, J., & Baozhong, M. (2018). Simulation on x-rays backscatter imaging based on Monte Carlo methods for security inspection. *Proceedings of SPIE*. Berlin, German: International Society for Optics and Photonics.
- ICRP. (2012). *ICRP statement on tissue reactions and early and late effects of radiation in normal tissues and organs - Threshold doses for tissue reactions in a radiation protection context*. ICRP Publication 118.
- ICRU. (1998). *Conversion coefficients for use in Radiological Protection against external radiation*. ICRU Report 57.

- Krzanovic, N., Zivanovic, M., Ciraj-Bjelac, O., Lazarevic, D., Ceklic, S., & Stankovic, S. (2017). Performance testing of selected types of electronic personal dosimeters in X- and Gamma radiation fields. *Health Physics*, 252-261.
- Lee, Y., Won, Y., & Kang, K. (2017). Performance test results of active personal doseimeters (APDS) used in nuclear power plant in Korea: A comparison with Thermo-luminescence doseimeters (TLDS). *Radiation Protection Dosimetry*, 431-437.
- Li, C., Zhang, J., Wang, W., & Chen, Y. (2019). Hydroxychloroquine combined with superficial X-ray - A new therapeutic method in the treatment of morphea profunda. *Dermatologic Therapy*, 1-3.
- MacKee, G. M. (1927). *Roentgen rays and Radium in the treatment of diseases of the skin*. Philadelphia: Lea & Febiger.
- Masterson, M., Cournane, S., McWilliams, N., Maguire, D., McCavana, J., & Lucey, J. (2019). Relative response of dosimeters to variations in scattered X-ray energy spectra encountered in interventional radiology. *Physica Medica*, 141-147.
- McCaffrey, J. P., Shen, H., & Downton, B. (2008). Dose rate dependency of electronic personal doseimeters measuring X- and gamma ray radiation. *Radiation Protection Dosimetry*, 229-235.
- NCRP. (2016). *Guidance on Radiation Dose Limits for the Lens of the Eye*. Bethesda, MD: National Council on Radiation Protection and Measurements.
- Ortega, X., Ginjaume, M., Hernandez, A., Villanueva, I., & Amor, I. (2001). The outlook for the application of electronic doseimeters as legal dosimetry. *Radiation Protection Dosimetry*, 87-91.

- Schneider, F., Clausen, S., Tholking, J., Wenz, F., & Abo-Madyan, Y. (2014). A novel approach for superficial intraoperative radiotherapy (IORT) using a 50 kV X-ray source: a technical and case report. *Journal of Applied Clinical Medical Physics*, 167-176.
- Sensus Healthcare. (2021, June 24). *Sensus Healthcare LLC*. Retrieved from SRT-100: <https://www.sensushealthcare.com/srt-100/>
- Sergei, S., Butorov, I., & Shevchenko, E. (2019). Monte Carlo modeling of a X-ray tube for superficial radiotherapy for evaluating the beam quality and the depth-dose distribution. *Journal of Physics*, 1-7.
- Sheu, R.-D., Powers, A., & Lo, Y.-C. (2015). Commissioning a 50-100 kV X-ray unit for skin cancer treatment. *Journal of Applied Clinical Medical Physics*, 161-174.
- Takata, N., Korosawa, T., & Tran, N. T. (2003). Angle dependence of signal currents from cylindrical ionisation chambers. *Radiation Protection Dosimetry*, 293-296.
- Texier, C., Itie, C., Serviere, H., Gressier, V., & Bolognese-Milsztajn, T. (2001). Study of the photon radiation performance of electronic personal dosimeters. *Radiation Protection Dosimetry*, 245-249.
- Thermo Fisher Scientific. (2021, June 23). *Radiation Detection and Instruments*. Retrieved from ThermoFisher: [thermofisher.com/epdtrdose](https://thermofisher.com/epdtrdose)
- Turner, J. E. (1995). *Atoms, Radiation, and Radiation Protection*. New York: John Wiley & Sons, Inc.
- Vigani, A., & Garcia-Pereira, F. L. (2014). Anesthesia and analgesia for standing equine surgery. *Veterinary clinics of North America: Equine practice*, 1-17.

## APPENDIX A

Table A1 - Data for the Detector Angular Response – Vertical

Exp Rate ( $\mu\text{R}/\text{min}$ )	0°	30°	45°	60°	90°
50 kV	68.0	64.0	65.3	66.0	70.7
70 kV	185.3	177.3	178.7	186.0	183.3
100 kV	440.0	420.0	420.0	426.7	420.0

Table A 2 - Data for the Detector Angular Response – Horizontal

Exp Rate ( $\mu\text{R}/\text{min}$ )	0°	30°	45°	60°	90°
50 kV	44.0	40.0	42.7	46.7	47.4
70 kV	126.7	124.0	130.7	134.7	138.6
100 kV	363.3	360.0	364.0	374.7	389.3

## APPENDIX B

Table B1 - Data for the Effect of Applicator Size on Exposure Rate experiment at 0 cm

0 cm	Exposure Rate (mR/hr)		
	50 kV	70 kV	100 kV
1.5	3.9	41	235
2	6.9	79	404
2.5	11	117	599
3	13	161	780
4	26	319	1620
5	37	319	2460
10	82	458	4120
CB8	64	600	3450
CB18	396	2880	7500

Table B2 - Data for the Effect of Applicator Size on Exposure Rate experiment at 50 cm

50 cm	Exposure Rate (mR/hr)		
	50 kV	70 kV	100 kV
1.5	1.2	5.8	27
2	1.4	9.4	46
2.5	1.8	14	74
3	2.5	18	95
4	4.2	37	193
5	7.2	65	292
10	15	102	447
CB8	13	94	444
CB18	39	238	780

## APPENDIX C

Table C1 - Data for the Scatter Heat Map Around SRT-100 experiment, 50 kV

Z=75	cm				X Axis								
		-2.5m	-2.0m	-1.5m	-1.0m	-0.5m	0m	0.5m	1.0m	1.5m	2.0m	2.5m	
	-2.0m	1.2	1.7	1.9	2.4	3.4	3.4	3.4	2.4	1.9	1.7	1.2	
	-1.5m	1.0	2.2	2.9	4.1	7.0	7.4	7.0	4.1	2.9	2.2	1.0	
	-1.0m	1.7	2.4	3.8	7.2	13.2	15.1	13.2	7.2	3.8	2.4	1.7	
Y Axis	-0.5m	1.9	2.6	5.0	12.0	25.0	30.0	25.0	12.0	5.0	2.6	1.9	
	0m	1.7	2.9	5.8	14.9	33.6		33.6	14.9	5.8	2.9	1.7	
	0.5m	1.9	2.6	5.0	12.0	25.0	30.0	25.0	12.0	5.0	2.6	1.9	
	1.0m	1.7	2.4	3.8	7.2	13.2	15.1	13.2	7.2	3.8	2.4	1.7	
	1.5m	1.0	2.2	2.9	4.1	7.0	7.4	7.0	4.1	2.9	2.2	1.0	
	2.0m	1.2	1.7	1.9	2.4	3.4	3.4	3.4	2.4	1.9	1.7	1.2	
Z=25	cm				X Axis								
		-2.5m	-2.0m	-1.5m	-1.0m	-0.5m	0m	0.5m	1.0m	1.5m	2.0m	2.5m	
	-2.0m	0.2	0.5	1.2	1.4	1.9	2.2	1.9	1.4	1.2	0.5	0.2	
	-1.5m	0.5	1.2	1.4	2.2	3.1	4.3	3.1	2.2	1.4	1.2	0.5	
	-1.0m	1.0	1.2	1.9	3.6	7.7	12.7	7.7	3.6	1.9	1.2	1.0	
Y Axis	-0.5m	0.7	1.4	2.4	6.0	23.3	76.8	23.3	6.0	2.4	1.4	0.7	
	0m	1.0	1.4	2.6	8.9	57.6		57.6	8.9	2.6	1.4	1.0	
	0.5m	0.7	1.4	2.4	6.0	23.3	76.8	23.3	6.0	2.4	1.4	0.7	
	1.0m	1.0	1.2	1.9	3.6	7.7	12.7	7.7	3.6	1.9	1.2	1.0	
	1.5m	0.5	1.2	1.4	2.2	3.1	4.3	3.1	2.2	1.4	1.2	0.5	
	2.0m	0.2	0.5	1.2	1.4	1.9	2.2	1.9	1.4	1.2	0.5	0.2	

## APPENDIX D

Table D1 - Data for the Scatter Heat Map Around SRT-100 experiment, 70 kV

Z=75	cm				X Axis								
		-2.5m	-2.0m	-1.5m	-1.0m	-0.5m	0m	0.5m	1.0m	1.5m	2.0m	2.5m	
	-2.0m	2.4	3.4	4.6	6.0	7.7	8.4	7.7	6.0	4.6	3.4	2.4	
	-1.5m	3.1	4.8	7.0	10.6	15.4	17.8	15.4	10.6	7.0	4.8	3.1	
	-1.0m	3.1	6.2	10.8	19.2	31.9	37.0	31.9	19.2	10.8	6.2	3.1	
Y Axis	-0.5m	3.6	7.0	13.7	28.6	72.0	88.8	72.0	28.6	13.7	7.0	3.6	
	0m	3.6	7.4	14.9	36.5	96.0		96.0	36.5	14.9	7.4	3.6	
	0.5m	3.6	7.0	13.7	28.6	72.0	88.8	72.0	28.6	13.7	7.0	3.6	
	1.0m	3.1	6.2	10.8	19.2	31.9	37.0	31.9	19.2	10.8	6.2	3.1	
	1.5m	3.1	4.8	7.0	10.6	15.4	17.8	15.4	10.6	7.0	4.8	3.1	
	2.0m	2.4	3.4	4.6	6.0	7.7	8.4	7.7	6.0	4.6	3.4	2.4	
Z=25	cm				X Axis								
		-2.5m	-2.0m	-1.5m	-1.0m	-0.5m	0m	0.5m	1.0m	1.5m	2.0m	2.5m	
	-2.0m	1.2	1.7	2.4	2.9	4.3	4.8	4.3	2.9	2.4	1.7	1.2	
	-1.5m	1.4	2.2	3.4	5.3	8.6	10.8	8.6	5.3	3.4	2.2	1.4	
	-1.0m	1.9	2.6	4.3	9.1	18.7	30.2	18.7	9.1	4.3	2.6	1.9	
Y Axis	-0.5m	2.2	3.4	6.7	15.8	69.6	192.0	69.6	15.8	6.7	3.4	2.2	
	0m	2.2	3.6	7.4	23.0	148.8		148.8	23.0	7.4	3.6	2.2	
	0.5m	2.2	3.4	6.7	15.8	69.6	192.0	69.6	15.8	6.7	3.4	2.2	
	1.0m	1.9	2.6	4.3	9.1	18.7	30.2	18.7	9.1	4.3	2.6	1.9	
	1.5m	1.4	2.2	3.4	5.3	8.6	10.8	8.6	5.3	3.4	2.2	1.4	
	2.0m	1.2	1.7	2.4	2.9	4.3	4.8	4.3	2.9	2.4	1.7	1.2	

## APPENDIX E

Table E1 - Data for the Scatter Heat Map Around SRT-100 experiment, 100 kV

Z=75	cm				X Axis							
		-2.5m	-2.0m	-1.5m	-1.0m	-0.5m	0m	0.5m	1.0m	1.5m	2.0m	2.5m
	-2.0m	4.3	7.7	9.6	12.7	17.0	17.5	17.0	12.7	9.6	7.7	4.3
	-1.5m	6.5	10.1	14.6	22.6	31.7	36.0	31.7	22.6	14.6	10.1	6.5
	-1.0m	8.4	13.0	23.3	38.4	72.0	84.0	72.0	38.4	23.3	13.0	8.4
Y Axis	-0.5m	8.9	14.6	28.1	62.4	141.6	182.4	141.6	62.4	28.1	14.6	8.9
	0m	17.8	16.1	30.2	81.6	194.4		194.4	81.6	30.2	16.1	17.8
	0.5m	8.9	14.6	28.1	62.4	141.6	182.4	141.6	62.4	28.1	14.6	8.9
	1.0m	8.4	13.0	23.3	38.4	72.0	84.0	72.0	38.4	23.3	13.0	8.4
	1.5m	6.5	10.1	14.6	22.6	31.7	36.0	31.7	22.6	14.6	10.1	6.5
	2.0m	4.3	7.7	9.6	12.7	17.0	17.5	17.0	12.7	9.6	7.7	4.3
Z=25	cm				X Axis							
		-2.5m	-2.0m	-1.5m	-1.0m	-0.5m	0m	0.5m	1.0m	1.5m	2.0m	2.5m
	-2.0m	2.9	3.8	5.3	7.4	10.3	11.3	10.3	7.4	5.3	3.8	2.9
	-1.5m	3.4	5.0	7.4	12.7	18.7	23.5	18.7	12.7	7.4	5.0	3.4
	-1.0m	3.8	6.0	10.6	21.6	41.3	72.0	41.3	21.6	10.6	6.0	3.8
Y Axis	-0.5m	4.8	7.9	13.9	35.5	146.4	388.8	146.4	35.5	13.9	7.9	4.8
	0m	4.8	7.9	17.8	48.0	309.6		309.6	48.0	17.8	7.9	4.8
	0.5m	4.8	7.9	13.9	35.5	146.4	388.8	146.4	35.5	13.9	7.9	4.8
	1.0m	3.8	6.0	10.6	21.6	41.3	72.0	41.3	21.6	10.6	6.0	3.8
	1.5m	3.4	5.0	7.4	12.7	18.7	23.5	18.7	12.7	7.4	5.0	3.4
	2.0m	2.9	3.8	5.3	7.4	10.3	11.3	10.3	7.4	5.3	3.8	2.9

## APPENDIX F

Table F1 - Data for Horse Phantom Backscatter Experiment at 0.5 m

<b>Exp Rate (mR/hr)</b>		<b>at 0.5m</b>	
<b>Angle</b>	<b>50 kV</b>	<b>70 kV</b>	<b>100 kV</b>
<b>0°</b>	74	170	331
<b>30°</b>	118	259	444
<b>60°</b>	127	266	446

Table F2 - Data for Horse Phantom Backscatter Experiment at 1 m

<b>Exp Rate (mR/hr)</b>		<b>at 1m</b>	
<b>Angle</b>	<b>50 kV</b>	<b>70 kV</b>	<b>100 kV</b>
<b>0°</b>	16	37	82
<b>30°</b>	28	67	113
<b>60°</b>	29	72	120

## APPENDIX G

Table G1 - Data for the Percentage Depth Dose using GafChromic Film for 1.5 cm applicator

1.5 cm	stance (mm)		
PDD	50 kV	70 kV	100 kV
100	0.0	0.0	0.0
90	1.0	1.1	2.0
80	1.8	2.8	3.8
70	3.0	4.4	6.0
60	4.2	6.3	9.0
50	5.5	9.0	12.0
40	7.3	12.1	14.2
30	9.1	15.1	17.3
20	11.0	18.4	22.2
10	15.8	25.1	31.6

Table G2 - Data for the Percentage Depth Dose using GafChromic Film for 2.0 cm applicator

2.0 cm	Distance (mm)		
PDD	50 kV	70 kV	100 kV
100	0.0	0.0	0.0
90	0.9	0.7	1.5
80	1.6	1.8	4.1
70	2.5	4.2	6.4
60	3.9	6.2	9.4
50	5.9	8.0	13.5
40	8.0	10.4	17.0
30	10.5	14.0	20.1
20	14.0	19.8	25.5
10	19.6	27.6	35.4

Table G3 - Data for the Percentage Depth Dose using GafChromic Film for 2.5 cm applicator

2.5 cm	Distance (mm)		
PDD	50 kV	70 kV	100 kV
100	0.0	0.0	0.0
90	1.0	1.7	1.6
80	1.9	3.1	3.9
70	3.0	4.8	6.0
60	4.5	6.8	8.1
50	6.0	9.0	12.2
40	7.7	12.2	16.0
30	10.1	15.9	18.5
20	12.5	19.9	24.3
10	18.0	27.0	35.3

Table G4 - Data for the Percentage Depth Dose using GafChromic Film for 3.0 cm applicator

3.0 cm	Distance (mm)		
PDD	50 kV	70 kV	100 kV
100	0.0	0.0	0.0
90	1.0	1.9	2.3
80	1.6	3.6	5.2
70	2.6	5.9	7.5
60	4.4	7.8	9.5
50	6.4	9.8	12.4
40	8.3	12.5	16.7
30	10.7	17.6	22.4
20	14.3	22.4	26.9
10	20.4	31.0	39.2

Table G5 - Data for the Percentage Depth Dose using GafChromic Film for 5.0 cm applicator

5.0 cm	Distance (mm)		
PDD	50 kV	70 kV	100 kV
100	0.0	0.0	0.0
90	1.1	1.8	2.4
80	1.9	4.2	4.0
70	3.2	5.7	6.4
60	5.0	7.1	8.9
50	6.6	8.9	12.7
40	8.2	11.5	16.4
30	10.4	16.6	19.7
20	12.5	22.3	26.0
10	17.8	32.5	36.3

## LIST OF ACRONYMS

BCC	Basal Cell Carcinoma
CFR	Code of Federal Regulations
CSK	Chronic Superficial Keratitis
CSU	Colorado State University
EPD	Electronic Personal Dosimeters
HDR	High Dose Rate
ICRP	International Commission of Radiation Protection
ICRU	International Commission of Radiation Units and Measurements
IORT	Intra Operative Radio Therapy
LINAC	Linear Accelerator
NRC	Nuclear Regulatory Commission
NVLAP	National Voluntary Laboratory Accreditation Program
OSL	Optically Stimulated Dosimeters
PDD	Percentage Depth-Dose
PMMA	PolyMethylMethAcrylate
RCO	Radiation Control Office
SCC	Squamous Cell Carcinoma
SRT	Superficial Radiation Treatment
SSD	Source to Skin Distance
SWP	Solid Water Phantom
TLD	Thermo Luminescence Dosimeters